HIGHWAY RESEARCH RECORD

Number 340

Asphalt Adhesion and Interfacial Phenomena

4 Reports

Subject Area

31 Bituminous Materials and Mixes

HIGHWAY RESEARCH BOARD

DIVISION OF ENGINEERING NATIONAL RESEARCH COUNCIL
NATIONAL ACADEMY OF SCIENCES—NATIONAL ACADEMY OF ENGINEERING

WASHINGTON, D.C. 1970

ISBN 0-309-01845-5

Price: $1.60

Available from

Highway Research Board
National Academy of Sciences
2101 Constitution Avenue
Washington, D.C. 20418

Department of Materials and Construction

R. L. Peyton, Chairman
State Highway Commission of Kansas, Topeka

R. E. Bollen and W. G. Gunderman
Highway Research Board Staff

BITUMINOUS DIVISION

Jack H. Dillard, Chairman
Virginia Department of Highways, Charlottesville

COMMITTEE ON EFFECTS OF NATURAL ELEMENTS
AND CHEMICALS ON BITUMEN-AGGREGATE COMBINATIONS
(As of December 31, 1969)

Herbert E. Schweyer, Chairman
University of Florida, Gainesville

Lester A. H. Baum
A. B. Cornthwaite
James R. Couper
Jack H. Dillard
Jack N. Dybalski
James L. Eades
A. W. Eatman
W. H. Gotolski
F. C. Gzemski
Rudolf A. Jimenez
L. C. Krchma
Da-yinn Lee
Robert P. Lottman
Kamran Majidzadeh
D. W. McGlashan
Robert E. Olsen
Ward K. Parr
J. Claine Petersen
L. L. Smith
Hans F. Winterkorn

Foreword

The 4 papers in this RECORD represent the results of research in the area of the interface among asphalts, water, and aggregate. These papers are an elaboration of material that was presented at a conference session on adhesion and interfacial phenomena at the 49th Annual Meeting.

Very little is known concerning the interactions that occur at the interfaces between asphalt and aggregates and any other atmospheric or environmental element that may enter the interface, and any type of contribution to this technology is welcome. These papers constitute a variety of viewpoints and techniques for considering such interactions. The material is quite varied in content and ranges from a consideration of the asphaltene component to consideration of composite combinations of polymeric materials as well as considerations of the interface between asphalt and aggregate in the presence of water.

Although at the moment the results may not be directly converted to pavement construction, they are valuable contributions to the technology in providing new viewpoints regarding such interfacial phenomena. It is hoped that more of this type of research will be undertaken, particularly that having applications to asphalt-aggregate mixtures.

—H. E. Schweyer

Contents

General Concepts of Adhesion

A. T. DiBENEDETTO, Department of Chemical Engineering,
Washington University, St. Louis

This paper presents a general review of concepts explaining the nature of adhesion at an interface between 2 condensed phases. The relationship between the surface energy of a solid and its theoretical tensile strength is explored. A molecular concept of surface energy is presented in which the relationships among intermolecular forces, surface tension, and work are discussed. A general description of interfaces and triple junctions and their relationship to contact angle wettability and adhesive bonding are then presented. Two examples of the effects of adhesion on the mechanical properties of composite materials are used to illustrate the importance of adhesion in multiphase systems.

•TO UNDERSTAND material behavior, one must examine structures at various levels. At a microstructural level, for example, the presence of voids, notches, grain boundaries, and other gross imperfections have effects on a number of important physical properties such as tensile strength, fracture toughness, and corrosion resistance. Many other properties are not dependent primarily on macroscopic flaws but rather depend on molecular structure and morphology. To understand properties such as yield strength, ductility, and diffusivity, one must examine the material at a crystallographic level (with tools such as X-ray diffraction and electron microscopy) where unit cell structures, dislocations, and other molecular defects can be observed. Still other properties such as electrical and thermal conductivity, magnetic susceptibility, and dielectric strength depend on the behavior of electrons, photons, phonons, and other subatomic particles.

This paper deals with properties that are, to one degree or another, dependent on the structural details of surfaces. As we will see, however, there are natural relationships between the so-called "surface" properties and the "bulk" properties of materials. If one considers physical properties from a molecular point of view, this is not at all surprising because the molecular properties of a surface must obviously be related to the molecules that make up the whole material.

As an illustration of this last point, let us consider the tensile strength of a brittle, elastic solid, where the theoretical limit of strength depends on the energy required to produce a fractured surface; i. e., it depends on the surface tension of the material.

Consider a unit thickness sheet in plane stress with a small crack, as shown in Figure 1. According to Griffith (9), the tensile strength of the sheet with a small microcrack is determined by the conditions that permit the crack to propagate through the cross section. The Griffith criterion for crack instability is that the crack will become unstable and the material will fail catastrophically when the free energy, G, of the material decreases with the crack size, i. e., $dG/d\ell \leq 0$. As the crack grows, strain energy, G_e, is released, $G_e = (\pi \ell^2 \sigma^2)/E$, and surface energy, G_s, is required to form the new surfaces, $G_s = 4\ell\gamma$, where σ is the external stress, E is the Young's modulus,

Paper sponsored by Committee on Effects of Natural Elements and Chemicals on Bitumen Aggregate Combinations and presented at the 49th Annual Meeting.

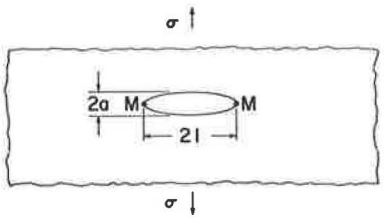

Figure 1. Elliptical microcrack causing maximum stress at M.

and γ is the surface energy per unit area. Hence, the Griffith criterion for fracture in plane stress is

$$\frac{\partial}{\partial \ell}(G_e + G_s) = -\frac{2\pi\ell\sigma^2}{E} + 4\gamma \leq 0 \qquad (1)$$

The theoretical breaking stress σ_b is, thus,

$$\sigma_b = \left(\frac{2E\gamma}{\pi\ell}\right)^{1/2} \qquad (2)$$

Equation 2 shows that the tensile strength of the sheet is determined by the surface energy of the solid, γ, the stiffness (or Young's modulus), E, and the size of the microflaw at which the break occurs.

In composite materials the importance of surfaces is magnified because of the fact that the behavior of composites also depends on the nature of the interfaces between filler and matrix. Tensile strength, fracture toughness, chemical resistance, and elastic moduli, for example, all depend on the degree of adhesion between phases. The degree of adhesion is, in turn, controlled by a number of physical and chemical factors. Among the former are surface area, surface roughness, degree of wetting, difference in moduli and Poisson's ratios, and differences in thermal expansion coefficients. Among the latter are differences in cohesive energies, polarities, surface energies, relative solubilities and susceptibilities to heat, oxidation, and hydrolysis. The strength of an interface will depend in a very complicated fashion on a combination of these factors.

In general, one may say that there is some theoretical maximum bond strength that can be developed under ideal conditions of perfect molecular contact, as shown schematically in Figure 2. The primary loss of strength is due to failure of the molecules

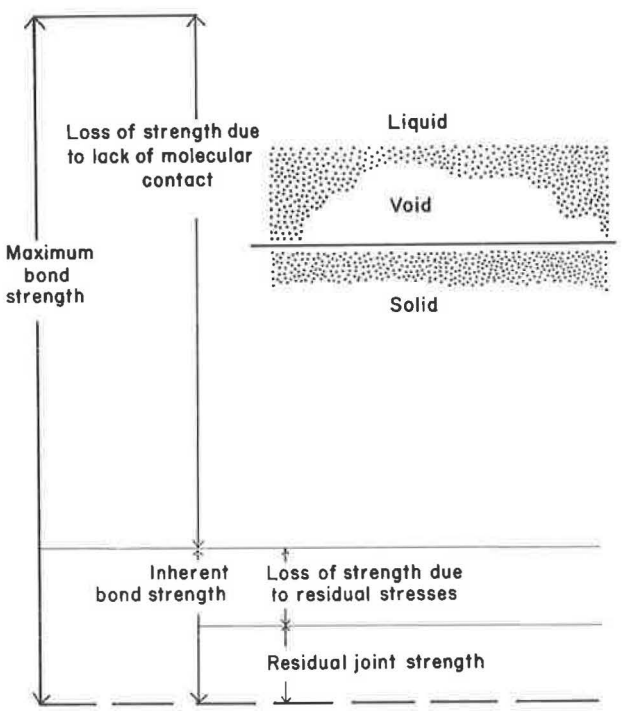

Figure 2. Factors affecting adhesive bond strength.

to approach their proper bonding distances of a few angstrom units. One may visualize this as a microvoid at the interface that is then capable of concentrating stress and causing premature failure. A second major loss in bond strength comes about from the development of residual stresses at the interface. Normally, a matrix or adhesive is applied in the fluid state and then solidified by cooling or chemical reaction or both. This invariably causes a differential shrinkage at phase boundaries that leads to undesirable stress concentrations. The net residual joint strength may be only a very small fraction (i.e., less than 1 percent) of the theoretical limit.

A MOLECULAR CONCEPT OF SURFACE ENERGY

When an atom or a molecule is in the bulk of a solid material, it is surrounded by a fixed number of nearest neighbors. In a crystalline solid with a closely packed cubic lattice, for example, each atom is surrounded by 12 nearest neighbors. Each molecule is thus constrained to vibrate in a "cage" of nearest neighbors. The thermal, or Brownian, motion of the atom will tend to keep it moving within the cage in a random fashion, while the intermolecular forces will tend to keep the atom constrained to its average lattice position at the center of the cage. This latter energy, called the potential energy of interaction, is approximately equal to the sum of the bond energies with nearest neighbors. Thus, the total potential energy of a given atom in a closely packed crystal lattice is roughly 12 times the bond strength between a single pair of atoms.

An atom in the free surface of a material has fewer nearest neighbors because it has essentially no near neighbors in the vapor phase. The missing interatomic bonds cause such an atom to have a smaller potential energy (i.e., less negative) than atoms within the bulk of the material. This "extra" energy relative to the bulk state is the surface energy of the material.

Surface energy is related to the work required to increase the area of a surface. Consider a unit area of soap film on a movable wire frame as shown in Figure 3. In order to hold the movable wire in place, a force of $2\gamma_{SV}$ dynes/cm of wire must be applied. In order to move the wire an infinitesimal amount, dx, to the left, an energy of $(2\gamma_{SV})(1)(dx)$ ergs must be expended. The total interfacial area increases in the process by an amount of $(2)(1)(dx)\,cm^2$. The energy expended per unit area of new surface formed is thus $2\gamma_{SV}dx/2\,dx = \gamma_{SV}$ ergs/cm^2 = γ_{SV} dynes/cm. Because more molecules are now at the surfaces, this process is equivalent to bringing some of the molecules from the bulk of the solid into the free surfaces, thus breaking a certain number of chemical bonds.

In this latter example, the surface energy has been equated to the mechanical work required to form a unit area of surface at constant temperature and pressure. This is numerically equivalent to the "Gibbs free energy" G_{SV} of the system

$$\gamma_{SV} = \Delta G_{SV} = \Delta H_{SV} - T\Delta S_{SV} = \Delta H_{SV} + T\left(\frac{\partial \gamma_{SV}}{\partial T}\right)_r \qquad (3)$$

For an isotropic fluid, there is a numerical equivalence between surface energy and surface tension. Because the most stable state of a material is one of minimum free energy (at constant temperature and pressure), isotropic fluids will tend toward a shape of minimum area per unit volume (i.e., a spherical shape). For anisotropic solids, the constraint of specific lattice geometry causes γ_{SV} to be orientation dependent because the surface energy will depend on the planar orientation of the crystal surface. This means that a spherical shape is not necessarily the most stable for a mass of anisotropic solids.

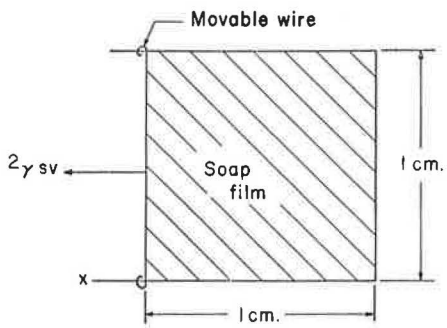

Figure 3. Illustration of surface tension.

INTERFACES

In the preceding section, the properties of free surfaces were discussed. These can also be considered as solid-vapor or liquid-vapor interfaces. Adhesive layers, inclusions in solids, grain boundaries in polycrystalline materials, or other similar situations are liquid-liquid, liquid-solid, and solid-solid interfaces. The properties of such interfaces can normally be described as triple junctions. A few illustrations are shown in Figure 4. Type a represents an inclusion of B in the grain boundary between 2 regions of material A. In the absence of a grain boundary in A, this would represent an inclusion B in a homogeneous matrix of A. Because surface energy and surface tension are synonymous in isotropic materials, the equilibrium state for the junction can be described by making a force balance about the point of intersection for the 3 regions.

$$\gamma_{AA} = 2\gamma_{AB} \cos\frac{\theta}{2} \tag{4}$$

where γ_{AA} is the tension in the A-A interface, and γ_{AB} is the tension in the A-B interface. For the case where A is homogeneous with no boundaries, $\gamma_{AA} = 0$ and $\theta = 180$ deg. Thus, if B is an isotropic fluid capable of attaining an "equilibrium" shape, it would take on a spherical shape in a homogeneous fluid matrix.

Figure 4b shows a triple junction, or meniscus, for liquid B in a capillary tube A. The case with a small contact angle, θ, represents good wetting of the capillary wall, while the case with a large contact angle represents poor wetting of the capillary wall.

Figure 4c shows a fluid drop, L, on a flat solid surface, S. Region V is either vapor or another liquid. The small contact angle represents good wetting, while the large contact angle represents poor wetting. At equilibrium,

$$\gamma_{SV} = \gamma_{SL} + \gamma_{LV} \cos\theta$$

or

$$\cos\theta = \frac{\gamma_{SV} - \gamma_{SL}}{\gamma_{LV}} \tag{5}$$

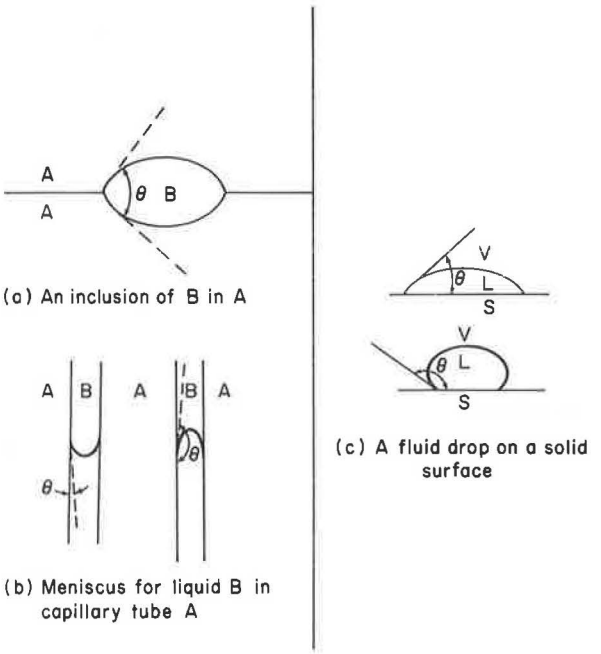

Figure 4. Triple junctions.

Equation 5 fixes the limits for absolutely no wetting and also for spontaneous wetting. If $\gamma_{SV} \geq \gamma_{LV} + \gamma_{SL}$, θ must be zero, and spontaneous wetting can occur. If $\gamma_{SL} \geq \gamma_{SV} + \gamma_{LV}$, θ must be 180 deg, which means that L cannot wet S to any extent.

Wetting is favored when the substrate is free of contamination (γ_{SV} is maximum), when the adhesive has an affinity for the substrate (γ_{SL} is low) resulting in a low interfacial tension, or when the surface tension of the adhesive is low (γ_{LV} is low). Surface roughness modifies the wetting characteristics because the fluid must move up and over asperities. For spreading on the rising side of an asperity, wetting is probably hindered, whereas on the falling side it is probably aided. Most important is the possibility of air being trapped under a spreading fluid, thereby changing the equilibrium contact angle. There is no accurate

way of predicting the net effects of roughness, but Wenzel has suggested that the equilibrium contact angle on a rough surface is given as

$$\cos\theta = r\frac{\gamma_{SV} - \gamma_{SL}}{\gamma_{LV}} \tag{6}$$

where r is the ratio of the true surface area to the mean plane surface area. Equation 6 suggests that, if θ is less than 90 deg, wettability is enhanced by roughness and, if θ is greater than 90 deg, wettability is hindered by roughness.

When a liquid spreads over a porous surface, it must wet the capillary passages in order to displace the air in the pores. In a cylindrical open pore of diameter d, the depth of penetration is equal to

$$\sqrt{\frac{\cos\theta\ \gamma_{LV}\ dt}{4\eta}}$$

where t is time and η is viscosity. Thus, as $\theta \to 90$, $r \to 0$, and $\eta \to \infty$, it takes a very long time to fill a pore. If the pore is closed at one end, the gas is merely compressed, trapping a void at the interface. Pore shape also affects the wettability. Filling a diverging cone, for example, requires an increasing surface energy as one moves to a wider section; thus, filling a diverging pore is not thermodynamically favored.

ADHESIVE BONDING ACROSS INTERFACES

There are several ways that 2 materials can interact across a phase boundary. The 2 most important types of bonding action can be classified as mechanical interaction and chemical interaction.

A mechanical interaction can be a geometrical effect where there is an interlocking of the 2 components across an interface. This type of action can be important when one of the substances is porous and the other can penetrate the pores and solidify. Adhesives for paper and wood may at least partially depend on this kind of bonding. A second type of mechanical interaction depends on a frictional resistance due to squeezing one component around an inclusion of the other. The shrink fitting of a wheel on a rim is a good analog for this type of action. In a composite material, differential thermal expansion can cause a "shrink fitting" around a rigid inclusion that can result in a significant compressive force on the inclusion and, thus, high "frictional adhesion." It can be shown that the compressive loading on an isolated filament in a glass fiber-epoxy composite can result in a frictional bond of 200 to 1,000 psi. In a heavily loaded composite, in which there are many fiber-fiber interactions, the stress fields around any one filament become extremely difficult to calculate accurately, and it is hard to say what the mechanical adhesion is. It is reasonably well accepted, however, that, if one wishes to have interfaces that are at least as strong as the constituent materials in shear, it is necessary to develop some kind of chemical bonding.

Chemical bonding at an interface is developed by wetting the solid surface with a fluid. Once molecular contact has been attained, the 2 phases can interact through intermolecular forces. The magnitude of the interaction depends on the type of chemical bonds formed.

Chemical bonding can be classified into primary and secondary bonding. Primary bonds, schematically shown in Figure 5, generally have bond energies of the order of 30 to 100 k-cal/g-mole and involve interatomic distances of 1 to 3 Å. This leads to theoretical strengths of the order of 10^6 to 10^7 psi. Primary bonding can be either ionic, covalent, or metallic. An ionic bond is an electrostatic interaction between highly electronegative (e.g., F) and highly electropositive (e.g., Na) atoms. When 2 such elements interact, the electronegative element draws an outer shell electron away from the electropositive element, thereby forming an anion and a cation. These will then coulombically interact to form an electrostatic bond, as shown in Figure 5a. A covalent bond is a true sharing of the electron orbitals of the interacting atoms as shown in Figure 5b. The outer shell electrons of such atoms lose their identity and

form molecular orbitals that bind the nuclei of the interacting atoms. This manifests itself as a high electron density along the internuclear axis. Metallic bonds are similar to covalent bonds in that outer shell electrons are shared by the nuclei of many atoms.

The effects of primary bonding are of importance to composites technology. The mixing of a metal matrix with a metal or oxide reinforcement often results in intermetallic compound formation at interfaces. Such reactions have a marked effect on the composite properties. Likewise, organic matrices can be chemisorbed onto surfaces, resulting in the formation of organic compounds at the interfaces. It is very likely, for example, that the glass-silane coupler-organic matrix interfaces involve some type of condensation reactions that in some cases result in cohesive interfaces, as shown in Figure 6.

Secondary, or Van der Waal's, bonds, shown schematically in Figure 7, generally have bond energies of the order of 0.5 to 10 k-cal/g-mole and involve interatomic distances of 3 to 5 Å. This leads to theoretical strengths of the order of 10^5 to 10^6 psi. These bonds are thus an order of magnitude weaker than primary bonds. Secondary bonding arises from electrostatic and inductive interactions among charges, dipoles, and multipoles in adjacent molecules or from London dispersion interactions (Van der Waal's forces) between molecules.

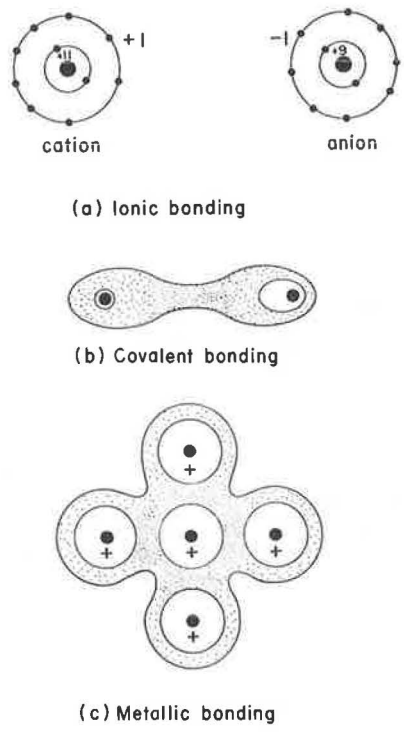

Figure 5. Types of primary chemical bonding.

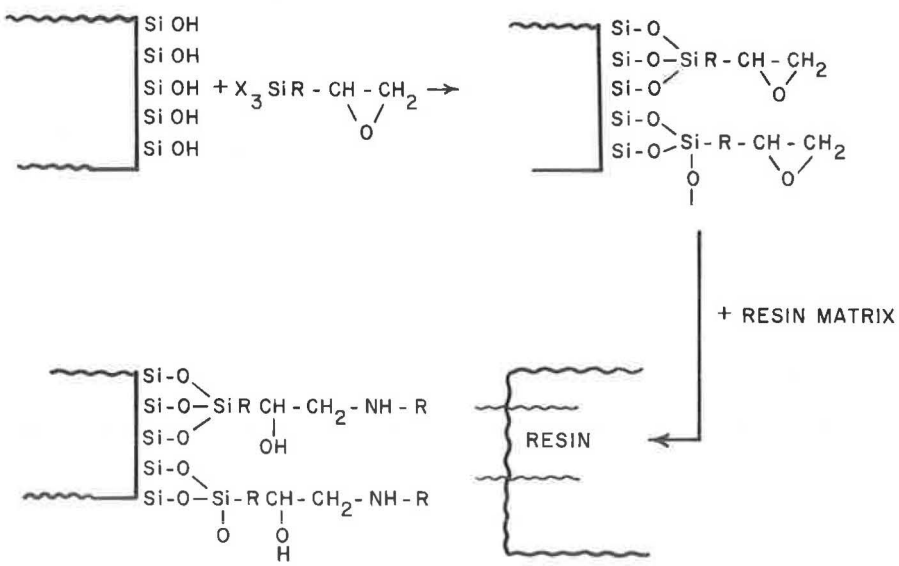

Figure 6. Coupling reaction at a glass-silane-epoxy interface.

Qualitatively, when 2 relatively simple molecules, separated by a distance r, interact in this manner, the potential energy of interaction can be represented by a function of the form

$$\phi_{12} = \frac{B}{r^m} - \frac{A}{r^n} = (-\phi_{12}^*)\left[\left(\frac{r^*}{r}\right)^m - 2\left(\frac{r^*}{r}\right)^n\right] \tag{7}$$

where the first term is a net repulsion and the second term is a net attraction. The quantities A and B are constants, m is constant at about 10 to 30, and n is constant at about 1 to 7, depending on the type of secondary bond. Equation 7 generally looks like the curve shown in Figure 8. The minimum represents the maximum interaction potential, and the distance at the minimum r* represents the most stable distance between particles.

The interaction energy between 2 materials across an interface and the tensile strength of the resulting adhesive bond can be related to intermolecular forces by considering the energy of adsorption of a single molecule A at a distance, d, from a solid surface, as shown in Figure 9.

The interaction between the molecule and an annular ring below the solid is $N_A\, 2\pi r\, dr\, dz\, \phi_{12}$ where N_A is the molecular density. One may integrate a potential function such as Eq. 7 over the whole solid to obtain the total energy of interaction of molecule A with the solid. If one then multiplies by the density of the adsorbed material, N_L, the total interaction energy can be estimated. To a zero order of approximation one can show that the maximum energy of adsorption for Van der Waal's bonding is given by

$$(\phi_{\text{adsorption}})_{\max} \rightarrow 2.5\, N_A\, N_L^{2/3}\, (\phi_{12}^*)(r^*)^3 \tag{8}$$

If one assumes that $r^* \rightarrow 3$ to 4 Å, $N_A \rightarrow N_B \rightarrow 4 \times 10^{22}$ particles/cc, and $\phi_{12}^* \rightarrow 0.3$ to 7.0 k-cal/g-mole, the energy of adsorption becomes $(\phi_{\text{adsorption}})_{\max} \rightarrow 60$ to 2,000 ergs/cm^2. Experimental data for the energy of adhesion of liquids to high-energy solids show that dispersion bonding results in energies of 100 to 200 ergs/cm^2.

Thus, we see that even with the very crude molecular model chosen here one may easily predict the proper order or

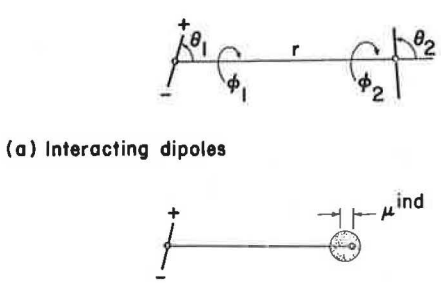

(a) Interacting dipoles

(b) Dipole can induce moments in other molecules

(c) London dispersion interactions occur even between neutral molecules

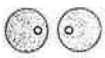

(d) When molecules come close together they repel

Figure 7. Secondary interactions.

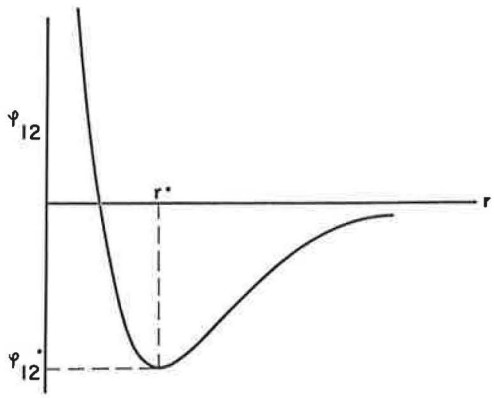

Figure 8. Schematic representation of the net interaction potential between 2 molecules.

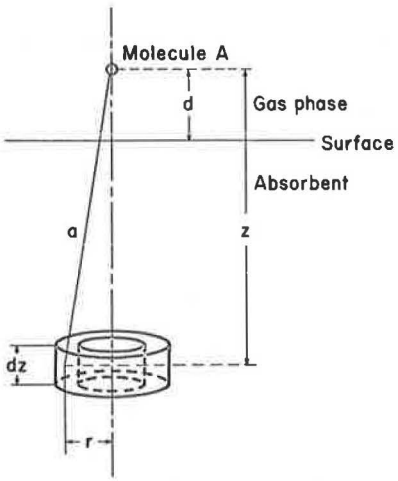

Figure 9. Interaction of a molecule with a plane surface.

magnitude for the energy of interaction for 2 materials in molecular contact across an interface.

Because the intermolecular force is related to the intermolecular energy by $f = -d\phi/dr$, one may also estimate a theoretical maximum tensile strength for the interface by differentiating Eq. 7 to obtain an equation relating force and interplanar separation and then by evaluating the force at the maximum where $df/dr = 0$. To a zero order of approximation it can be shown that

$$f\,max \rightarrow 4.5\ r^{*2}\ N_A\ N_L^{2/3}\ \phi_{12}^{*} \qquad (9)$$

Using the same numbers as before for the molecular constants, one obtains a theoretical maximum tensile strength of $f\,max \rightarrow$ 60,000 to 1,500,000 psi. Experimental data show that the actual tensile strength of an interfacial bond rarely exceeds 200 to 2,000 psi. Thus, we see that the actual tensile strength of an interfacial bond is only a small fraction of the theoretical bond strength.

Because the energy calculations were reasonable, one can assume that, if wetting and molecular contact are attained at an interface, even relatively weak Van der Waal's forces should give a strong, cohesive interface. The low mechanical strength is thus controlled by factors other than molecular cohesion. In real composite materials, the phases are not always compatible, and wetting and molecular contact are not necessarily attained. The low mechanical strength of an interface is most certainly caused by microscopic and submicroscopic defects. Probable causes of such defects will include imperfect wetting, shrinkage on solidification, thermal stresses, dirty surfaces, and cracks and voids in the interfacial layer. One of the challenges of composites technology is to overcome these defects through improved fabrication techniques.

Because of a lack of knowledge of intermolecular forces combined with an uncertainty of the true nature of any given interface, one cannot readily predict the properties of an interface a priori. A practical method of analysis can be developed, however, by combining the concept of intermolecular forces with a knowledge of the thermodynamic properties of surfaces.

The total intermolecular potential energy of interaction between an adhesive and an adherent is merely a measure of the work of adhesion between the 2 bodies and is, therefore, related to the surface tension at the interface. Figure 10 shows the relationship between the surface free energies and the work of adhesion.

$$-\phi_{ads} = W_A^{\circ} = \Delta G_{T,p} = \gamma_A + \gamma_B - \gamma_{AB} \qquad (10)$$

In this case the work of adhesion is related to the surface free energies of the 2 solids in a vacuum. Likewise, the specific cohesion of a solid can be represented by

$$W_c^{\circ} = \Delta G_{T,p} = 2\gamma_A \qquad (11)$$

This equation, schematically shown in Figure 10, shows that the work required to break a solid along a specific crystallographic plane is equal to the free energy required to form the 2 free surfaces in a vacuum. When solid-solid interfaces are broken in the presence of air, the free energies of the surfaces in the presence of an absorbed film of air are used rather than the surface energies in vacuum. More importantly, one is often interested in the work required to pull a liquid away from a solid surface, leaving the equilibrium adsorbed vapor film on the surface. Then, Eq. 10 is written as

$$W_A = \gamma_{SV} + \gamma_{LV} - \gamma_{SL} \qquad (12)$$

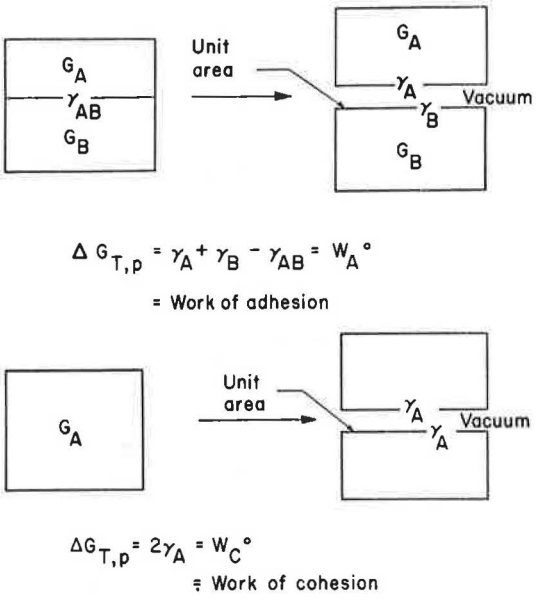

Figure 10. Schematic representation of relation between surface free energies and work.

where the subscripts S and L replace A and B and γ_{SV} and γ_{LV} are the surface free energies of the solid and liquid respectively for surfaces in equilibrium with the saturated vapor. The use of Eqs. 5, 10, and 12 gives

$$W_{\mathring{A}} = W_A + (\gamma_S - \gamma_{SV}) = \gamma_{LV}(1 + \cos\theta) + \pi_e \tag{13}$$

In Eq. 13, the work of adhesion $W_{\mathring{A}}$ is the work required to break a unit area of solid-liquid interface in vacuum, producing solid-vacuum and liquid-saturated vapor interfaces. The quantity π_e is the change in free energy accompanying the immersion of a film-free solid in a saturated vapor. It is often referred to as the equilibrium film pressure of the adsorbed vapor film.

The heat of immersion, H_i°, can be measured calorimetically by placing a powdered solid in an evacuated container, immersing the container in a fluid within a calorimeter, breaking the container, and monitoring the accompanying energy change. The free energy change may be expressed as

$$\Delta G_i = \gamma_{SL} - \gamma_S = \gamma_{LV} - W_{\mathring{A}} = \Delta H_i^\circ + T\left(\frac{\partial \Delta G_i}{\partial T}\right)_p \tag{14}$$

The enthalpy of immersion is, thus,

$$\Delta H_i^\circ = \gamma_{LV} - W_{\mathring{A}} - T\left(\frac{\partial \gamma_{SL}}{\partial T}\right)_p + T\left(\frac{\partial \gamma_S}{\partial T}\right)_p \tag{15}$$

The enthalpy of adhesion, $\Delta H_{\mathring{A}}$, may be similarly defined as $W_{\mathring{A}} - T\left(\frac{\partial W_{\mathring{A}}}{\partial T}\right)$, so that the heats of immersion and adhesion are related by

$$\Delta H_i^\circ = \gamma_{LV} - T\left(\frac{\partial \gamma_{LV}}{\partial T}\right)_p - \Delta H_{\mathring{A}}^\circ = \Delta H_{LV} - \Delta H_{\mathring{A}} \tag{16}$$

Thus, one may obtain the enthalpy of adhesion by subtracting the measured enthalpy of immersion from the total surface enthalpy of the liquid (because heats of immersion are generally negative, the enthalpy of adhesion is generally larger than the surface enthalpy of the liquid).

Experimental measurements of contact angles, equilibrium film pressures, heats of immersion, and interfacial tensions can be used as quantitative measures of the molecular interaction at an interface. Conversely, it should be possible to estimate these properties from knowledge of the intermolecular forces. Although we do not have enough analytic information to make accurate predictions, it is possible to make reasonable estimates of these properties on a number of simple systems by combining elementary dispersion force theory with experimental data on the surface tensions of the pure components.

EFFECTS OF ADHESION ON THE MECHANICAL PROPERTIES OF COMPOSITES

Let us consider 2 examples of the effects of interfacial bonding in order to illustrate the importance of adhesion and surface properties to the mechanical behavior of composites.

Consider first the yield strength of glass-reinforced polyphenylene oxide (PPO) composites. An untreated glass surface has little adhesion to PPO. Treatment of the glass surface with γ-amino propyltriethoxysilane (A-1100) makes it capable of some bonding to the plastic. Figures 11 and 12 show the improvement in strength directly attributable to the improved bonding with glass bead and with E-glass fiber reinforcement respectively. Figures 13 and 14 show electron scanning microscope pictures of a small portion of the fracture surfaces of the PPO-glass bead composites. Figure 13 shows a typical situation for untreated beads, where the plastic has easily pulled away from the glass surfaces, leaving the beads sitting in large craters on the surface. Figure 14 shows the improvement in adhesion, where the plastic stays in contact with the surface until voids form away from the interface and propagate inward. Figure 15 shows a transmission electron photograph of the interface between an A-1100 treated glass bead and the adhering matrix. It is clear that the response of the matrix to the propagating crack front is considerably different in the vicinity of the interface. There exists a layer of about 7,000 Å in thickness that is seemingly oriented relative to the glass surface. This is an indication that viscous flow has not occurred in this region.

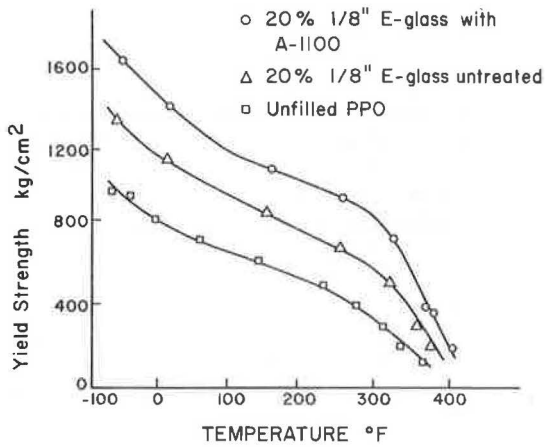

Figure 11. Yield strength for glass fiber random reinforced PPO.

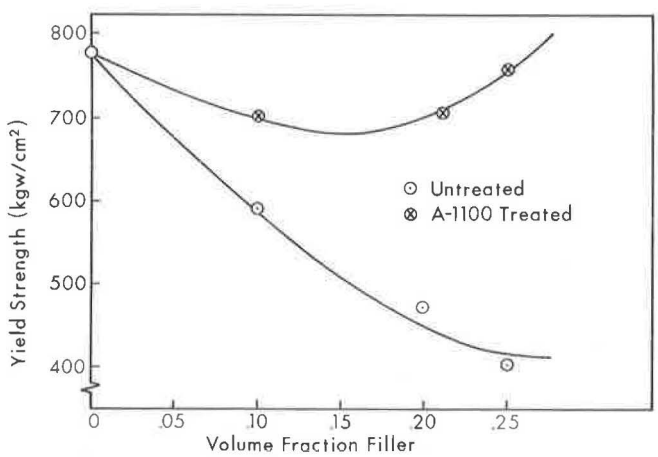

Figure 12. Effect of surface treatment on strength of glass bead-PPO composites.

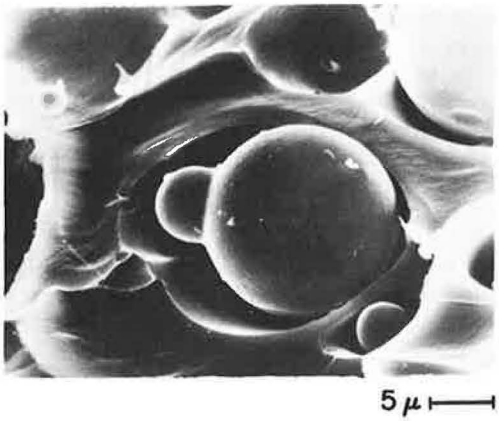

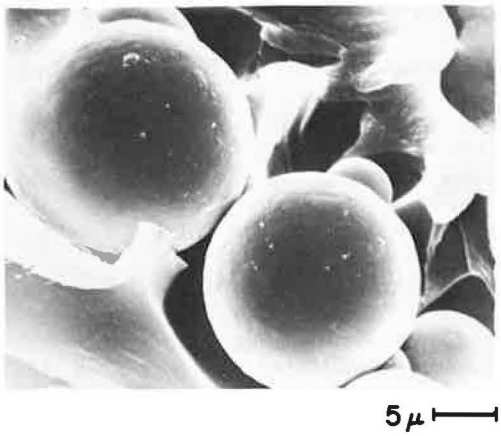

Figure 13. Fracture surface of a 10 percent by volume untreated glass bead-PPO composite.

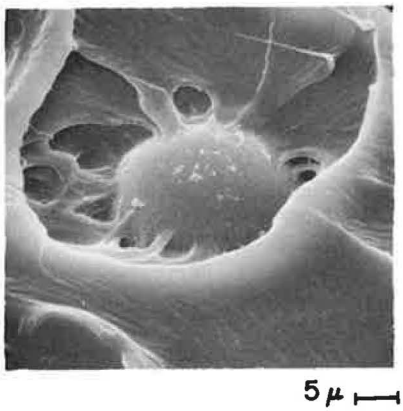

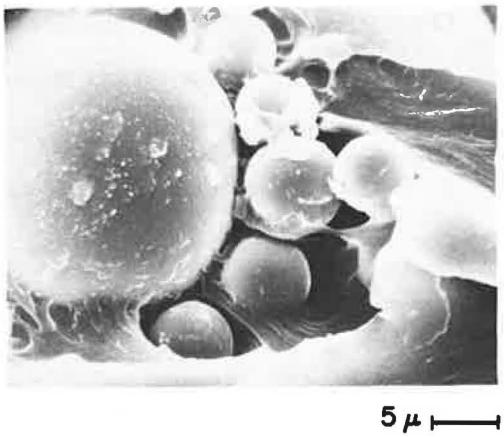

Figure 14. Fracture surface of a 10 percent by volume A-1100 treated glass bead-PPO composite.

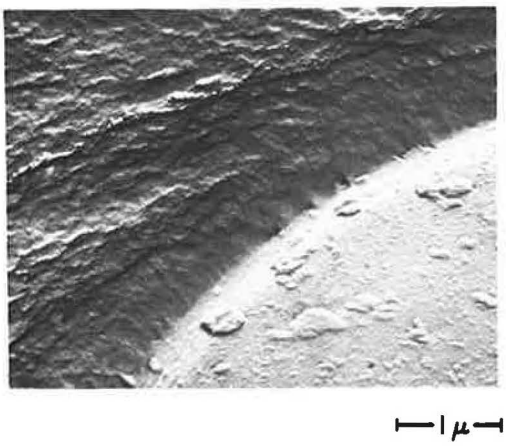

Figure 15. Transmission electron photograph of the PPO-glass bead interface of an A-1100 treated composite (fracture surface replica).

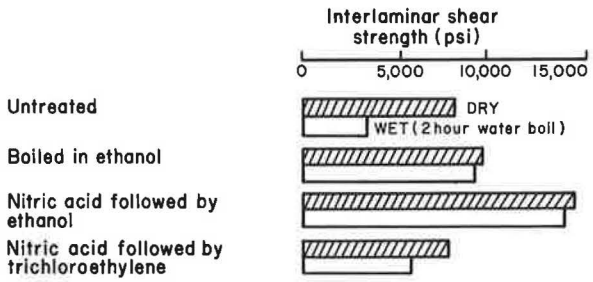

CONTACT ANGLE OF EPON 828 ON BORON FILAMENTS (JONES & PORTER ref.)

Untreated	27-30°
After hot ethanol	7
After trichloroethylene	14

Figure 16. Effects of surface treatments on boron-epoxy composites.

A most important nonmechanical function of an adhesive interface in a composite is the protection of the surfaces of the high strength fibers from chemical attack and physical damage. If the matrix does not wet the fiber, it can accomplish neither of these. As an illustration, consider the effects of surface treatment on boron fibers (Fig. 16). The finite contact angles indicate a lack of spontaneous wetting. A treatment with hot ethanol, however, promotes the best wetting conditions. Because boron and boron oxide surfaces have high energy, 25 times higher than the epoxy resin, the lack of spontaneous wetting probably indicates the presence of dirt and other impurities. An untreated surface thus gives a weak bond and poor resistance to boiling water. The poor resistance to boiling water is probably indicative of the solubility of boron oxide in water. Boiling in ethanol probably removes the boron oxide and partially cleans the surface, leading to better strength and strength retention. Etching in nitric acid followed by boiling in ethanol gives the most complete surface cleaning and thereby gives the best strength and strength retention.

REFERENCES

1. Chemistry and Physics of Interfaces. American Chemical Soc., Washington, D.C., 1965.
2. Zisman, W. A. Industrial and Engineering Chemistry, Vol. 55, No. 10, 1963, pp. 19-38.
3. Clark, F., Rutzler, J. E., and Savage, R. L., eds. Adhesion and Adhesives: Fundamentals and Practice. John Wiley and Sons, New York, 1954.
4. Davies, J. T., and Rideal, E. K. Interfacial Phenomena. Academic Press, New York, 1961.
5. Gomer, R., and Smith, C. S., eds. Structure and Properties of Solid Surfaces. Univ. of Chicago Press, 1953.
6. Adams, N. K. The Physics and Chemistry of Surfaces. Oxford Univ. Press, London, 1941.
7. Mykura, H. Solid Surfaces and Interfaces. Dover Publications, New York, 1966.
8. Weiss, P., ed. Adhesion and Cohesion. Elsevier Publishing Co., New York, 1962.
9. Griffith, A. A. Philos. Trans., Royal Soc., London, Series A, Vol. 221, 1920-21, p. 163.

Pressure-Induced Stripping in Asphaltic Concrete

ROBERT P. LOTTMAN and DENNIS L. JOHNSON, University of Idaho

The purpose of this paper is to present a case for a significant stripping mechanism based on thermally induced pressure in the void water of saturated asphaltic-concrete mixtures. Although observations and measurements are obtained from asphaltic-concrete pavement and laboratory specimens representing typical asphaltic concrete in southeastern Idaho, the mechanism could also be prevalent in other states. Possible quantitative mechanisms are outlined for using the concept of activating void water pressure and resisting adhesion strength. It was found that void water pressures may develop to 20 psi under differential thermal expansion of the compacted asphaltic concrete and could exceed the adhesion strength of the binder-aggregate interface. Void water entrance to the interface was observed for all cases of stripping in the form of pinholes connected to void fissures. The voids (or fissures) are developed in the compaction phase of asphaltic-concrete production and are normally of the "correct" size to enable saturation. However, they are still of low enough permeability to enable the creation of void water pressures during temperature change. The problem discussed is one of the moderately weak asphalt-aggregate interface, depicting instances where static stripping tests are not illustrative of stripping potential and, consequently, some interfacial stressing is required.

•THE INTERACTION of water and asphaltic concrete may under particular circumstances cause stripping or loss of adhesion and consequential detachment of the asphalt from the aggregate. The result of this action decreases the cohesive strength of the mixture until it has no inherent structural strength as a paving material and it approaches the condition of compacted gravel.

Because asphaltic concrete is a nonhomogeneous material, many factors can contribute to the overall stripping problem. Built-in porosity and permeability allow water to enter the mixture and flow through the void paths. The type of asphalt cement and the surface characteristics of the aggregates are responsible for adhesive strength; the adhesive strength may not be adequate in the presence of internal water.

Although much research is being done on the stripping problem, more recent investigations have been made on compacted asphaltic mixtures. It was found in previous Idaho experimentation that the use of compacted-mixture specimens in the testing program is a more direct approach than use of loose asphalt-aggregate mixtures. This is because internal void water or pore pressures, for example, can be created realistically in compacted-mixture specimens, producing forces that tend to strip the mixtures. It is hypothesized that these pressures, similar to those in actual Idaho pavements, either cause or appreciably accelerate stripping when the asphalt-aggregate interface is weak.

The objective of this paper, therefore, is to formulate the stripping mechanism as occurring in Idaho pavements by using test results obtained in the laboratory and observations made in the field.

Paper sponsored by Committee on Effects of Natural Elements and Chemicals on Bitumen-Aggregate Combinations and presented at the 49th Annual Meeting.

A recent study was made to determine the extent of stripping in Idaho (1). Pavement samples from throughout the state were taken and examined for stripping in both the +4 and -4 sieve size of aggregate particles. The major conclusion made from the study was that no single mixture or location factor appeared to be responsible for the observed stripping. Quartzite, sandstone, and limestone were the most frequent aggregates identified with stripping. This study pointed out the widespread nature of the stripping problem and the need for identifying the mechanism of stripping in the case that a nonapparent combination of 2 or more factors is responsible.

A special study group was formed on the West Coast to examine stripping in problem aggregates from Idaho and Arizona. Using conventional test procedures on loose aggregate, each of the cooperating agencies tested and reported on the stripping potential of these aggregates. Idaho's Inkom aggregate, which did show stripping in a highway pavement, is of interest here.

A summary of action taken so far by the group may be found in the minutes of the May 16, 1969, meeting (2). Testing in Arizona, California, Oregon, and Washington indicated that the Idaho aggregate would be suitable for use under present standards.

California research indicates that the Inkom aggregate is not susceptible to stripping as determined by conventional test methods on both loose and compacted mixtures (3). The immersion-compression tests showed a small (not serious) amount of stripping. It was attributed to the presence of about 5 percent montmorillonite in the aggregate fines.

Thus several agencies, acting independently, have shown the Inkom aggregate not to be susceptible to stripping. Yet the pavement constructed with this aggregate has shown extensive stripping failure. It was felt that a different approach was needed to more fully simulate field conditions because external or internal water action may not have existed in a realistic form in the conventional tests.

Freeze-thaw or temperature cycling as a method for measuring resistance to stripping has not yet been used for water-saturated asphaltic mixtures. However, Parr of the Michigan Department of State Highways some time ago mentioned the possibility of freeze-thaw breakup in asphaltic concrete. The destructive effects of freezing on portland cement concrete have been known for some time, and Powers in 1945 postulated the existence of destructive hydraulic pressures generated by an advancing ice wall (4). It was thought that the formation of ice on the outside of the concrete and the subsequent expansion of the ice would drive unfrozen water into the permeable voids under high pressure, thus causing tensile failure of the cement mortar.

The possibility of air pore pressures in nonsaturated asphaltic concrete undergoing temperature rise was advanced by Jones (5). He found that thermal coefficients of expansion were, on the average, larger than corresponding coefficients of contraction. He concluded that air pressures in the voids were causing creep of the mixture during a given temperature rise. If no vacuum formed in the voids on the contraction part of the cycle, lack of "reverse" pressure would show smaller coefficients of contraction. Jones did not attempt mathematical calculation of this effect because of the complexity of the situation.

Lee and Nichols have mentioned the possible existence of hydraulic pore pressures in pavement surfaces caused by the "pumping" action of moving vehicle wheels (6). They surmise that water will creep between the asphalt binder and the aggregate under this pumping action and, as a result, will cause debonding or stripping. Their approach was essentially centered around surface failure of pavements in the presence of water.

Measurement of thermally induced hydraulic pore pressures in soils has been performed by Plum and Esrig (7). They tested undrained clays in a triaxial cell with a lateral confining pressure of 30 psi at 57 F. By raising the temperature of the cell to 95 F, they noted a corresponding pore pressure increase to 45 psi. Additional cycles of thermal rise and fall between these 2 temperatures resulted in further increases of pore pressure to a maximum of 48 psi and eventually a closed hysteresis loop. This work serves as an example of existence and measurement of internal pore pressure induced thermally in a porous material and may be analogous to a saturated asphaltic concrete.

Research and testing to date on the causes of stripping have centered on thermodynamic theoretical aspects of adhesion failure and on surface energy measurements and tests related to those concepts. A series of conventional tests on Inkom aggregate failed to reveal the full potential stripping nature of this aggregate. It appears that compacted mixtures subjected to freeze-thaw or other thermal cycling could be used in a test method for predicting stripping in asphaltic concrete.

Based on the literature investigated and reviewed, it was believed that an approach to measure hydraulic void (pore) pressures in compacted, water-saturated asphaltic mixtures and to relate this pressure to stripping would be promising.

STRIPPING CAUSED BY FREEZE-THAW CYCLING

Most research performed on stripping of asphaltic concrete is aimed at preventing failure. This research project began as an examination of a pavement near Pocatello, Idaho, using Inkom aggregate (BK142-S) and already showing stripping failure, in an attempt to identify the failure mechanism. Duplication of the failure was essential before identification of the mechanism could begin. Because freeze-thaw action in saturated portland cement concrete often causes failure, extreme freeze-thaw cycles of 0-120-0 F were tried as a possible means of duplicating the field failure of asphaltic concrete. Use of freeze-thaw appears to be a reasonable simulation of field conditions in spring and fall when temperatures vary widely and pavements are most likely to be water-saturated.

Testing by freeze-thaw cycling showed extreme stripping under full saturation, some under partial saturation. No stripping was observed in dry specimens under similar conditions or when the specimens were saturated but not freeze-thaw cycled. A vacuum-saturation technique was developed to completely saturate test specimens. Vacuum-saturated specimens subjected to 21 cycles of freeze-thaw showed the same type of failure as samples of pavement taken from the field. A freeze-thaw stripped specimen containing Inkom aggregate is shown with the actual pavement sample in Figures 1 and 2. The photographs show an abundance of bare aggregate particles in the larger sizes. Appearance of the outside of failed specimens is normal with no indication of stripping, but cohesive strength of these specimens is very low.

Having seemingly duplicated the field failure mode by using freeze-thaw, it was decided to use this test to indicate the stripping potential of control specimens. Inkom aggregate was chosen as the main test aggregate. It contained 74 percent quartz, 5 percent montmorillonite, 5 percent mica (illite), 5 percent calcite, and traces of iron oxide, dolomite, and talc (3). It was considered to be dense-graded. Another aggregate, Washington No. 28 (nonstripping), was used for a very limited number of specimens. Five specimens using asphalt cements A, B, and C and 2 specimens using another asphalt were made with Inkom aggregate at 4.94 percent asphalt content

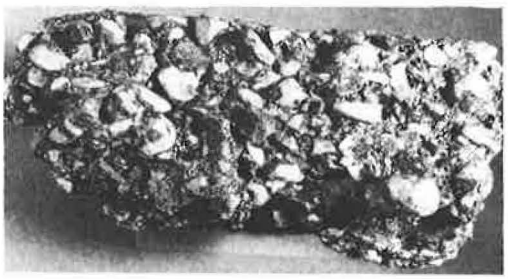

Figure 1. Field specimen showing stripping in actual pavement.

Figure 2. Laboratory-duplicated specimen showing stripping after freeze-thaw cyclic test.

(aggregate basis). This asphalt content was the resultant average of extractions performed on actual pavement samples. All specimens received identical treatment during the mixing and compacting procedure. After vacuum-saturation, 1 specimen was opened without cycling (0 cycles). The others were opened at 3, 9, 15, and 21 cycles. Amount of stripping was visually estimated as percentage of total area believed to be bare aggregate.

The amount of stripping was found to increase proportionally to the number of cycles, but specimens having undergone only a few cycles of freeze-thaw still showed significant stripping or adhesion failure. The specimens showed many completely bare larger sized aggregate particles covered with a film of water. In almost all cases a socket with very smooth sides was left where the aggregate particle came out. Other bare aggregates could be pulled out easily and cleanly from their sockets.

Several variations from the control asphalt-aggregate combination were made and cycled in the same manner as the control specimens. In the following list of the different or variant features, the first six incorporate Inkom aggregate:

1. All minus No. 200 aggregate was dry sieved out,
2. All minus No. 200 aggregate was washed out,
3. All minus No. 200 aggregate was washed out by using detergent soap in the wash water and then washing out detergent,
4. Gradation was changed from 39 to 25 percent passing No. 10 sieve,
5. Four different chemicals were added at 2 percent of the weight of the asphalt cement,
6. Asphalt content was raised from 4.94 to 6 percent, and
7. Washington No. 28 aggregate was used at design asphalt content of 6.2 percent of aggregate weight.

For most of the 7 cases, 2 specimens were prepared, saturated, freeze-thaw cycled, and then examined for stripping at 9 and 21 cycles.

These results indicate possible trends in the effects of these variations on stripping of the Inkom aggregate mixture. Good improvement in resistance to stripping was noted for one of the additives, but the others provided no significant improvement. Specimens made by using the Washington No. 28 aggregate showed a significant lack of stripping, probably because of the type of basalt aggregate surface itself, being porous and pitted, and chemically different as compared to the smooth-surfaced Inkom aggregate.

There was no improvement in stripping resistance due to mixture changes under variations 1, 2, 3, 4, and 6. Variations 1, 2, and 3 are quite similar in that they all had reduced amounts of material passing the No. 200 sieve. All specimens were quite weak and porous due to the lack of fines acting as a filler. Removal of the fine dust in variation 1 did not appreciably decrease the severity of stripping. When washing or detergent washing accompanied the dust removal as in variations 2 and 3, significant stripping still occurred but there seemed to be fewer completely bare aggregates.

Reduction of the percentage of aggregate passing the No. 10 sieve in variation 4 had an effect that was similar to the effect of variation 1. The mixture was porous and weak, and significant stripping occurred.

Increasing the asphalt content in variation 6 had the effect of reducing the porosity or void ratio well below the usual values (1.5 to 4 percent versus previous values of 4 to 8 percent). This reduced the amount of water entering the specimen, keeping some specimen areas entirely dry. Significant stripping was still prevalent, but it was not found in these dry areas where the asphalt content within the specimen, due to internal variation, was high.

Thus, it appeared that "conventional remedies" were not generally successful for bringing the Inkom aggregate mixture up to the stripping resistance of a nonstripping mixture such as the one made with Washington No. 28 aggregate. Research work is continuing in Idaho on the specific problem.

Present testing has also shown that warm-cool thermal cycles, such as 40-110-40 deg, also produce or accelerate stripping in the same manner as described with the freeze-thaw cycling.

INDICATIONS OF VOID WATER PRESSURE

The idea that void water pressure was causing failure came about as a result of a routine examination of freeze-thaw stripped mixtures under 7- to 30-power magnification. It was noticed that, when test specimens were slowly pulled apart at warm temperatures, many bare aggregate particles left smooth-sided sockets as they came out of the mixture. Examination of these sockets through the stereomicroscope revealed that the asphaltic binder pulled cleanly away from the aggregate particle, making the socket a mirror image of the aggregate particle surface. In almost all sockets there were also seen small pinholes or void paths leading to the asphalt-aggregate interface from the asphalt binder matrix.

Based on these visual observations, a conception of the situation at a typical void is shown in Figure 3. This void situation is entirely hypothetical because it is not known how the voids and void paths are arranged. This representation is based on observations and accumulated knowledge of the Inkom asphaltic mixture. It is hypothesized that water from the void paths in the asphalt binder matrix under hydrostatic pressure enters the interface of the asphalt binder and the aggregate particle. Then the water under pressure proceeds through the interface, displacing the binder, until the aggregate surface is coated by a thin film of water. Observations of specimens from freeze-thaw cycle tests showed entire aggregates surrounded by a film of water.

Photographs of an interfacial displacement and a resulting socket are shown in Figures 4 and 5. Visible are the void pinholes and crevices in the socket where interfacial water entry was made. The texture of the walls is about the same as the surface of the Inkom aggregate shown.

Similar sockets are observed in failed portland cement concrete specimens. The mode of failure for concrete is interfacial aggregate bond failure in these cases and is thought to be produced by tensile forces. It is hypothesized that such tensile forces can be present in porous, saturated, compacted asphaltic mixtures and are responsible for this stripping action.

TEMPERATURE-INDUCED VOID WATER PRESSURE

Typical asphaltic concretes are purposely designed with a small percentage of air voids to allow for differential thermal expansion of asphalt cement. Supposedly, these voids prevent the asphalt cement from being flushed onto the pavement surface during thermal expansion. Unfortunately these air voids may become saturated with water from rain, snowmelt, and even vapor condensation due to the rise of water vapor in the subgrade or subbase. A temperature rise after this saturation can cause expansion of the free water trapped in the mixture voids, possibly resulting in significant void pressures when the voids are saturated.

Because asphaltic concrete is permeable, water could flow out of the void spaces under the pressure developed by the temperature rise and, in time, relieve the pressure developed. Thus, the temperature rise probably causes pressure increase and some time-dependent pressure relief in the void pressure. Qualitative aspects and measurements are discussed in this section.

Knowledge of the way in which water behaves in the void paths of compacted asphaltic concrete is very difficult to obtain. Gross measurements must be relied on for data while the actual results are being caused by many microactions with the material. Consider the typical void situation shown in Figure 3. After a temperature rise, the following changes may be expected to occur in the saturated mixture:

1. Asphaltic-concrete mixture expands and tends to increase the size of the voids,
2. Asphalt cement expands and tends to decrease the size of the voids, and
3. Water expands in the voids and tends to increase the size of the voids.

For gross measurements, a rough value for cubical thermal expansion of asphaltic concrete is 7×10^{-5}/deg F (5), while that for water is 12×10^{-5}/deg F, a somewhat larger value. Expansion values for pure asphalt cement are about 3×10^{-4}/deg F (5). Thus, it may be assumed that there is not enough room available for expansion of the water and asphalt cement into mixture voids.

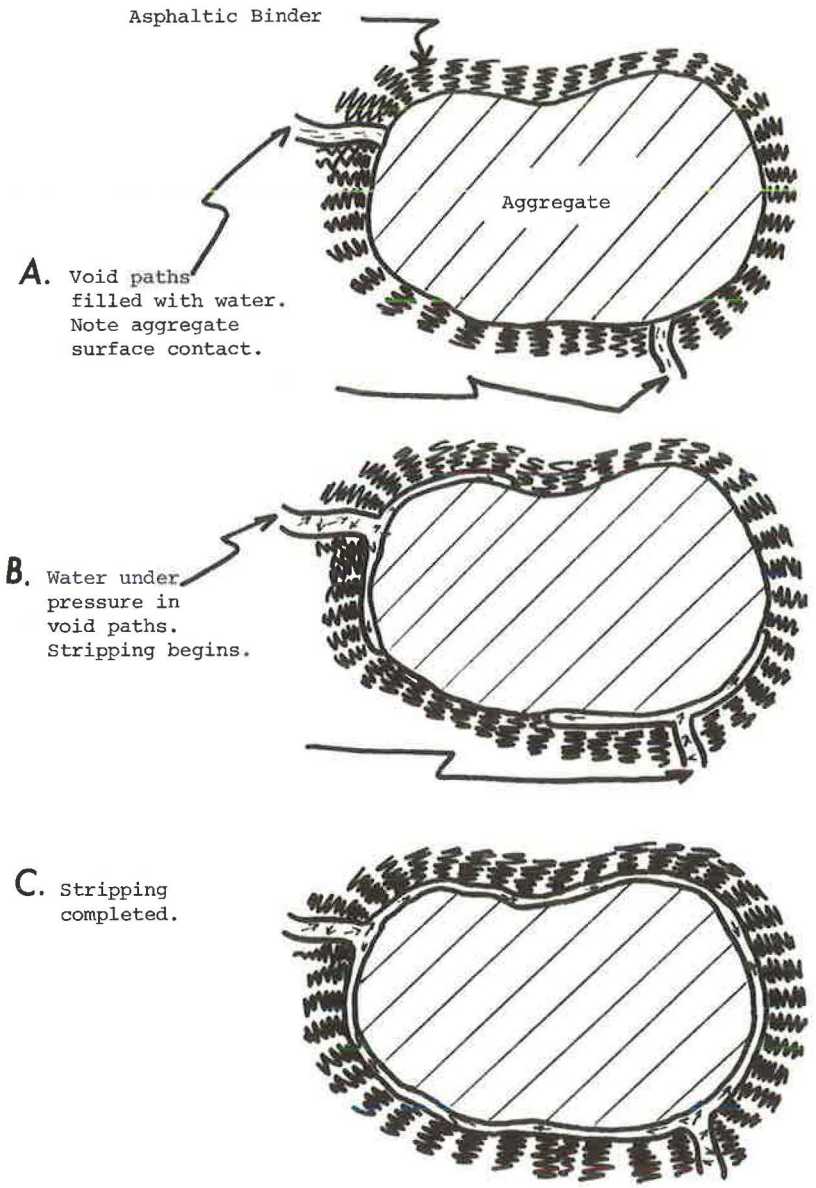

Figure 3. Hypothesized void pressure mechanism.

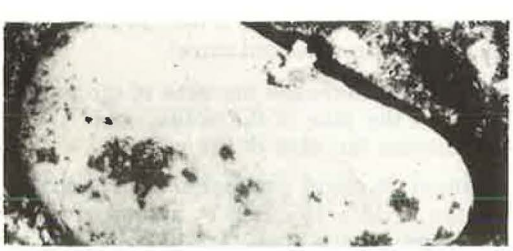

Figure 4. Typical binder-aggregate interfacial displacement.

Figure 5. Displacement socket in binder.

If the asphalt cement expands just enough to fill the expanding mixture, then this will cancel out any change in the volume of voids. Volume expansion of the water will produce void pressure in the water and tensile stress in the mixture. The water under pressure attempts to flow out of the void area. If the permeability is high enough, then the water will physically leave the mixture; if not, then the tensile stress resulting from the pressure may break adhesion bonds and the water, in contact with parts of the aggregate surface, could flow around aggregates causing stripping.

The pressure inside a porous mixture would cause expansion of the mixture dictated by the tensile bulk modulus of the mixture. This slight volume strain would tend to lower the pressure. However, the quantitative aspect of how both volume strain and permeable flow would act together to dissipate some or all of the pressure developed was not investigated.

An indirect method of void pressure analysis may be explained by considering the physical situation of an asphaltic-concrete specimen being subjected to hydrostatic pressure in the void area. Such a pressure would cause the mixture to expand slightly. Volumetric expansion could be measured either by direct volume change or by measurement of axial strain and conversion to volumetric strain through use of Poisson's ratio. Volumetric strain of the mixture may also be stated as the result of a "tensile" pressure stress divided by the tensile bulk modulus of the mixture. Internal pressure can be calculated if both bulk modulus and volumetric strain are known. On the other hand, if strains are small, internal pressure can be calculated if axial modulus and axial strain are known. This will be subsequently discussed.

Bulk modulus may be found from Young's elastic modulus by the following equation:

$$K = \frac{E}{3(1 - 2\mu)}$$

where

K = bulk modulus, psi;
E = elastic or axial modulus, psi;
μ = Poisson's ratio.

Thus, an experiment yielding data from which E is calculated may also be used to find values for K providing μ is also known.

Asphaltic concrete is a viscoelastic material, and its response must be considered in this light. Generally if the application of the modulus constants is of very short duration, only the elastic constants will be necessary to describe the material's response. If the application is long term, then time-dependent or viscoelastic constants are necessary. Modulus values in this case were to be used for calculation of stress (void pressure) induced by a temperature change. The exact manner in which void pressure changes with time is not known and, therefore, the time base for the modulus is also unknown. Consequently, an average value of E was calculated, determined from E at the instant of unloading (elastic) and after 10 sec of loading (viscoelastic) on cylindrical specimens. These 2 values were averaged to yield an E with time-dependent and with some time-independent properties.

The tensile, axial modulus values are shown in Figure 6. Actual data points were scattered, and the plots represent average values determined by regression analysis.

Axial strains were used with the axial modulus to calculate the internal pressure by using the following relationship:

$$\epsilon_V = 3\epsilon(1 - 2\mu)$$

where

ϵ_V = volumetric strain;
ϵ = axial strain; and
μ = Poisson's ratio.

If the bulk modulus relationship is used, then

$$\text{Pressure} = \epsilon_V K = 3\epsilon(1 - 2\mu)\frac{E}{3(1 - 2\mu)}$$

or

$$\text{Pressure} = E_\epsilon$$

The strain was considered to be the additional strain of a saturated specimen as compared to a similar but dry specimen.

Axial strains were measured through the use of waterproof strain gages attached to specimen pairs of the same void ratio and asphalt type and content. One specimen of the pair was kept dry by a wax costing; the other was vacuum saturated. Each pair was placed in a water bath, and their axial strain differences were monitored as the water bath temperature was changed. Therefore, during a temperature rise, positive strain indicates that the saturated specimen has a height increase relative to the dry one. Void pressures were calculated by using the previous equation with the axial modulus and axial differential strain at a particular temperature.

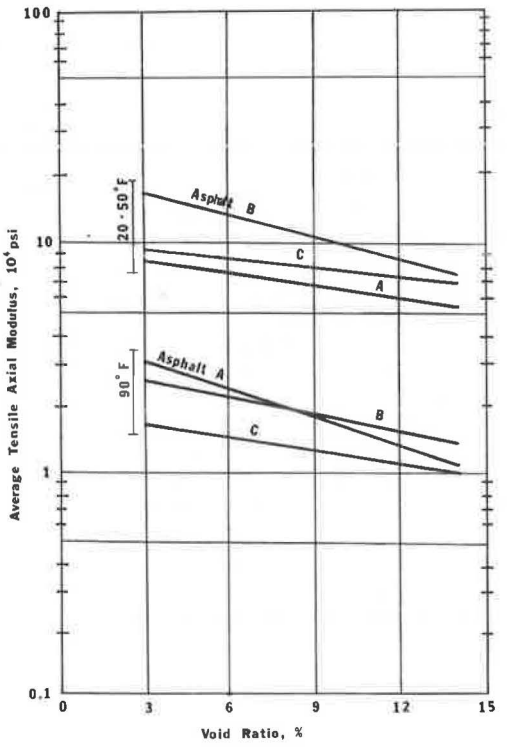

Figure 6. Axial moduli of compacted Inkom asphaltic mixture.

This approach was used on 4 pairs of specimens made with Inkom aggregate and asphalt A, and 3 pairs made with asphalts B and C. All pairs of samples were tested at the same time in the laboratory water bath, and temperature increments of approximately 20 F were used from 10 to 110 F with 12 hours between the temperature increments (generally similar to the freeze-thaw test conditions). Strains for each pair were read at the end of each 12-hour period.

Calculated void pressures are shown in Figures 7 and 8 for asphalts A and B used in making the specimens. Two pairs showed negative strains and, therefore, "negative" pressures.

One possible explanation for the negative differential pressures is the influence of the specimen area where the 2 layers of compaction meet. This area is centrally located perpendicular to the specimen's longitudinal axis and direction of strain measurement. It is possible in some specimens that this area is not as dense as the rest of the specimen. It absorbs more water and, thus, could contain large amounts of ice at the low temperatures used. At the base temperature the saturated cylinder would have been slightly expanded because of the ice expansion. When the ice melted, the asphaltic concrete might have crept back together, thus indicating a negative strain in this temperature range.

The positive differential pressures shown in Figures 7 and 8 indicate no trends based on void ratio. All the void pressures peaked in the 50 to 70 F range because of the influence of the temperature-dependent axial modulus. Although during the test the strains usually increased, the axial modulus decreased more rapidly, resulting in lower pressures. It is interesting to note that the peak pressure occurred near the annual mean of the temperature range usually experienced in actual pavement. This could indicate more stripping in this part of the temperature range.

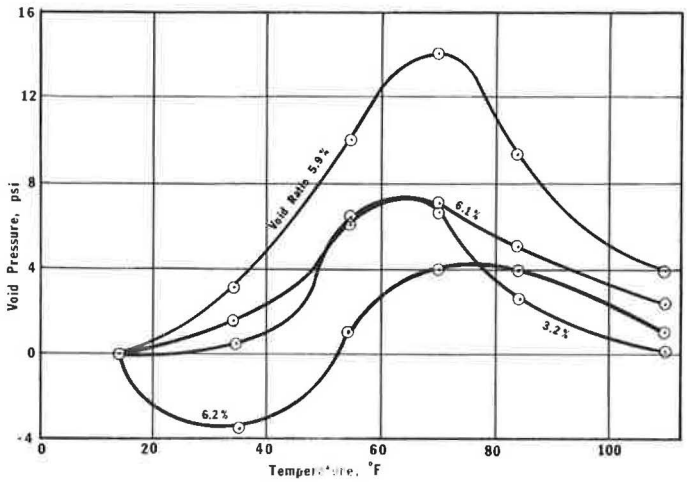

Figure 7. Void water pressure s temperature for asphalt A.

ANALYTICAL APPROACHES OF FAILURE MECHANISM

From a basic point of view, it would be desirable to predict the stripping potential from basic physical constants of the asphaltic binder, the aggregate, and the resulting mixture. Surface energy or adhesion strength of the asphalt-aggregate interface could be equated to maximum void pressure through quantitative use of an activating-resisting mechanism. Failure would be defined as the condition when activation or destructive forces exceed the resistive forces of the mixture bonds. Resistive forces could be made to exceed activating forces through experimentation with asphalt type, chemical additives, aggregate type, and other factors influencing asphalt-aggregate interfacial adhesion strength.

The following are 3 possible methods for such an analysis based on stripping caused by internal void pressure (internal tensile stress).

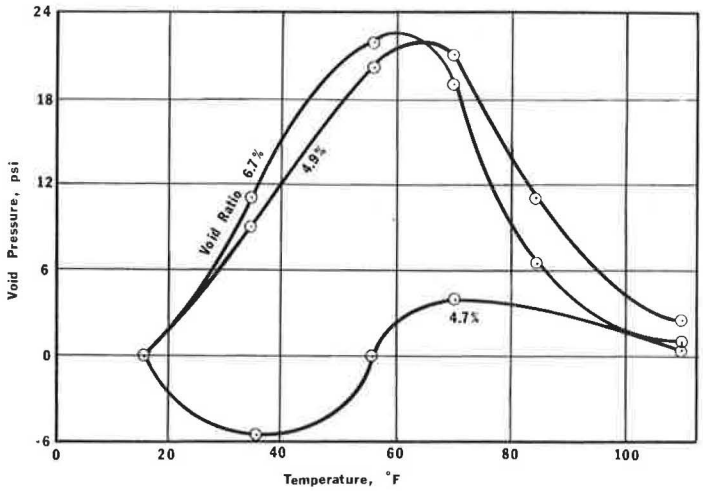

Figure 8. Void water pressure versus temperature for asphalt B.

Method 1—Activating-Resisting Forces With Mixture Properties

Consider a compacted asphaltic mixture that is saturated. Assume that a void pressure is produced by thermal expansion and that this pressure creates an internal hydrostatic tensile stress in the mixture. Let the activating force to cause stripping be equal to the product of the wetted surface area of the permeable voids and the void pressure. Let the resisting force to inhibit stripping be equal to the product of the aggregate surface area that is contacted by the "voidless" asphaltic binder and of the adhesion strength of the binder-aggregate interface.

Stripping will occur if the activation force is greater than the resisting force. Stripping could also occur even if the activating force is equal to the resisting force if a cyclic or fatigue void pressure loading is produced because of thermal change.

The activating force is as follows:

$$F_a = (Aw/V)P_v$$

where

F_a = activating force per unit volume of mixture;
Aw/V = wetted surface area per unit volume of mixture (a function of permeability and voids); and
P_v = void pressure.

The Appendix contains an explanation of Aw/V and a figure for estimating Aw/V versus voids for the Inkom mixture.

The resisting force is as follows:

$$F_r = (Ai/V)P_a$$

where

F_r = resisting force per unit volume of mixture;
Ai/V = surface area of bonded aggregate per unit volume of mixture; and
P_a = adhesion strength of binder aggregate interface.

Ai/V can be determined from the gradation and specific gravity of bonded aggregate. P_a can be determined from adhesion tests in the laboratory.

For the single-cycle case, stripping failure occurs when $F_a > F_r$. The following is an example for the Inkom mixture.

If there are 6 percent voids and asphalt A is used, then Aw/V = 200 cm^2/cm^3 of mixture (Fig. 9). If P_v = 14 psi (Fig. 1), then

$$F_a = [200(cm^2/cm^3)]\ 14\ psi\ (1\ in.^2/6.45\ cm^2)$$

$$(16.4\ cm^3/1\ in.^3) = 7{,}100\ lb\ tension/in.^3\ of\ mixture$$

Ai/V is calculated from the Inkom gradation with an SG = 2.60 for the aggregate. Assume that all minus No. 200 aggregate particles in the gradation are mixed with the asphalt A to form a "voidless" asphaltic binder that bonds to the plus No. 200 aggregate particles. Therefore, Ai/V = 39 $cm^2/1\ cm^3$ of mixture. (Note: If the minus No. 200 aggregate particles were not a part of the binder but were actually a part of the bonded aggregate in the mixture, then Ai/V would be about twice as large. Therefore, the resisting force would be twice as large.)

P_a is estimated to be 60 psi at 70 F and at 80-micron film thickness of binder (8). The binder in this case is considered to be asphalt plus the minus No. 200 filler. The 70 F temperature is about the temperature where the maximum void pressure, P_v, was found (Fig. 7). Then,

$$F_r = [39(cm^2/cm^3)]\ 60\ psi\ (1\ in.^2/6.45\ cm^2)$$

$$(16.4\ cm^3/1\ in.^3) = 5{,}950\ lb\ tension/in.^3\ of\ mixture$$

Because $F_a > F_r$, then stripping will occur in a single cycle.

Suppose we examine F_a versus F_r at higher and lower temperatures than 70 F. At 120 F, $P_v \rightarrow 1.5$ psi (Fig. 7) and, therefore,

$$F_a = (200)(2)(1/6.45)(16.4/1) = 1{,}020\ lb/in.^3\ of\ mixture$$

$$P_a \rightarrow 8.5\ psi\ (8)$$

$$F_r = (39)(8.5)(1/6.45)(16.4/1) = 840\ lb/in.^3\ of\ mixture$$

Thus, $F_a > F_r$ at 120 F, and stripping would also occur in this temperature range.

For 40 F, $P_v \rightarrow 5$ psi (Fig. 7) and, therefore,

$$F_a = (200)(5)(1/6.45)(16.4/1) = 2{,}540\ lb/in.^3\ of\ mixture$$

$$P_a \rightarrow 100\ psi\ (8)$$

$$F_r = (39)(100)(1/6.45)(16.4/1) = 9{,}900\ lb/in.^3\ of\ mixture$$

Thus, $F_a \ll F_r$ at 40 F, and stripping would not occur in this lower temperature range. Hence, the critical temperature range seems to be the middle range from 50-85 F.

It should be emphasized again that stripping is fatigue-like in character; and, even though $F_a = F_r'$, stripping could occur if F_a is repeated in a cyclic fashion. This is hypothesized from test observattions of the cyclic tests performed in this research.

Method 2—Activating-Resisting Hydrostatic Stress

In this method, stripping failure is assumed to depend only on the magnitudes of void pressure, the tensile stress at the asphalt binder-aggregate interface, and the adhesion strength of the interface. An activating-resisting relationship is as follows:

$$F_a' \gtrless F_r'$$

where

F_a' = activating stress, and

F_r' = resisting strength.

$$F_a' = P_v + T_h$$

where

P_v = hydrostatic pressure in saturated voids, and

T_h = equivalent hydrostatic or isotropic tensile stress at interface.

$$F_r' = P_a$$

where

P_a = adhesion strength at interface.

For a given compacted, saturated asphaltic mixture, F_r' is constant, and the condition at verge of stripping at constant temperature is

$$F_r' = F_a' = P_v + T_h$$

The freeze-thaw test produces equal P_v and T_h values because hydrostatic or isotropic tensile stress conditions exist. For example, at 70 F, the Inkom mixture with asphalt C (Fig. 8) contains a void pressure, P_v, of 18 psi in the 5 to 6 percent void range. This condition also produces an isotropic tensile stress, T_h, at the interfacial area of 18 psi. Therefore, $F_a' = 18 + 18 = 36$ psi. Stripping was also observed in a pure hydrostatic pressure test on the same mixture when $P_v = 35$ to 40 psi and $T_h = 0$. This indicates that $P_v + T_h$ could be equal to a constant, F_a', for a given mixture and leads one to believe that the sum of any test combination of P_v and T_h that equals 36 psi or greater should produce stripping in the mixture. Further tests to date have been inconclusive.

Method 3—Fracture Surface Work

A possible method is generally outlined based on an analogy with fracture mechanics. Here one would equate the stored elastic energy (activation) to the fracture surface work required to strip or displace the binder-aggregate interface (resistance).

Let the stored elastic energy be

$$E_a = (\sigma^2/2E)$$

where

E_a = elastic energy per unit volume of mixture;
σ = internal equivalent tensile stress; and
E = elastic modulus of the mixture.

And let the fracture surface work be

$$E_r = \gamma(\Delta A/\Delta V)$$

where

E_r = displacement surface work per unit volume of mixture;
γ = fracture surface energy area; and
$\Delta A/\Delta V$ = area of interface displaced per unit volume of mixture, which would equal A_i/V as defined in method 1.

σ would need to be measured directly, or indirectly as indicated previously in the experimental results shown in Figures 7 and 8. E is an experimentally determined elastic modulus for the compacted saturated mixture. γ is an experimentally calculated fracture surface work term depicting the resistance of the asphalt binder to completely displace from the aggregate surfaces. All would need to be measured at the given temperature desired.

Displacement or stripping would occur if $E_a > E_r$ under one loading of σ. If there is a cyclic effect, then stripping would be possible if E_a were about equal to E_r as suggested in method 1.

Summary of Methods

The methods outlined would be possible means for predicting stripping susceptibility or resistance. Probably methods 1 and 3 would lend themselves more to a basic approach using engineering or scientific units. However, empirical evaluation based on outcomes of freeze-thaw tests, for example, would provide quicker results considering the pressing need for an acceptable test method especially in Idaho. Unfortunately the empirical evaluation test does not directly provide information as to what is happening within the mixture or as to the basic importance of mixture variables.

CONCLUSIONS

The following conclusions are based on test observations to the end of 1969:

1. Characteristics and severity of stripping in pavements incorporating Inkom aggregate can be duplicated with laboratory-made, vacuum-saturated, compacted, asphaltic-mixture specimens exposed to cyclic freeze-thaw test generally in the range of 0-120-0 F.

2. Stripping appears to be produced by internal surging of water pressure in the voids of the mixture. It is developed primarily through differential thermal expansion of asphaltic binder, asphaltic mixture, and void water.
3. Stripped aggregate particles are surrounded by a film of water that has displaced the asphaltic binder. It is hypothesized that stripping will occur when there is contact between the aggregate surface and an initial path of void water. Initial paths in the binder sockets of stripped aggregate particles are always observed.
4. The freeze-thaw or thermal cyclic test can also be used as an evaluation test as well as a conditioning test. After cycling, laboratory personnel can slowly pull apart the tested specimens at 120 F and visually observe the severity of stripping. The test is immediately more useful than analytical approaches, but it does not provide basic mechanistic information.
5. As observed via the cyclic test, some chemical additives in the asphalt considerably reduce the stripping; some do not. Tests so far indicate no significant improvement in stripping resistance due to treating the aggregate by conventional methods. A change of aggregate type, i.e., the nonstripping Washington No. 28, produced mixtures that had only a small degree of stripping.

ACKNOWLEDGMENTS

The results and implications discussed in this paper were derived from a research project sponsored by the Idaho Department of Highways and the Federal Highway Administration. The opinions, findings, and conclusions expressed in this paper are those of the authors and not necessarily those of the sponsoring agencies.

REFERENCES

1. Hatch, L.M. Field Determination of the Areal Extent of Stripping in Idaho's Pavements. Idaho Department of Highways, Boise, Aug. 1969.
2. Finn, F.N. Minutes of Meeting of Study Group for Asphalt Stripping in Asphalt Concrete. Pacific Coast Div., The Asphalt Institute, San Francisco, May 16, 1969.
3. Chechetini, J. Stripping Chracteristics of an Aggregate Source From Idaho. Materials and Research Dept., California Division of Highways, memorandum, file 19107-641139, Oct. 29, 1968.
4. Powers, T.C. A Working Hypothesis for Further Studies of Frost Resistance of Concrete. ACI Jour., Proc. Vol. 41, Feb. 1945, p. 245.
5. Jones, G.M., Darter, M.I., and Littlefield, G. Thermal Expansion-Contraction of Asphaltic Concrete. Proc. Assn. of Asphalt Paving Technologists, Vol. 37, 1968, p. 56.
6. Lee, A.R., and Nicholas, J.H. Adhesion in the Construction and Maintenance of Roads. In Adhesion and Adhesives Fundamentals and Practice, John Wiley and Sons, New York, 1954.
7. Plum, R.L., and Esrig, M.I. Some Temeprature Effects on Soil Compressibility and Pore Water Pressure. HRB Spec. Rept. 103, 1969, p. 231.
8. Lottman, R.P. The Moisture Mechanism That Causes Stripping in Asphalt Pavement Mixtures. Dept. of Civil Eng., Univ. of Idaho, Moscow, First Annual Rept. of Research Proj. 73-51, Nov. 1968.
9. Johnson, D.L. Debonding of Water-Saturated Asphaltic Concrete Caused by Thermally Induced Pore Pressure. Univ. of Idaho, Moscow, MSCE thesis, Sept. 1969.
10. Lottman, R.P., and Johnson, D.L. The Moisture Mechanism That Causes Stripping in Asphaltic Pavement Mixture. Dept. of Civil Eng., Univ. of Idaho, Moscow, Second Annual Rept. of Research Proj. 45-302 (73-51), Dec. 1969.
11. Vallerga, A.B. Development of Water Permeameter for Asphalt Concrete Cores. Material and Research Development, Oakland, Calif., final report, Jan. 1966.
12. Young, R.N., and Warkentin, B.P. Introduction to Soil Behavior. Macmillan Company, 1966.

Appendix

TEST AND ESTIMATING PROCEDURES

Water Permeability Tests

Falling-head permeability tests were performed on vacuum-saturated, compacted, asphalt concrete specimens. Voids in each specimen were varied.

Reference to the falling-head permeability test can be found in most soil mechanics books. We used 100 in. of head at the beginning of each test. This head was found to be insufficient to drive water through those specimens at voids lower than 4 percent; therefore, our results are repeated for specimens having voids greater than 4 percent.

Careful preparation of mixture specimens was necessary because it was found that permeability was sensitive to slight mixture variations. In the beginning of the tests, specimens from the same mixture produced permeabilities of 100 percent or more in difference at the same void content. Weight blending of aggregate sized fractions, close control of oven temperature, asphalt content, and compaction were all required to reduce this variation.

Specimens, 4 in. wide by 5 in. high, were thinly coated on their sides (except ends) with paraffin to fill in surface voids. Two or 3 coatings of thermosetting resin were applied following the paraffin coating. After the coatings hardened, the ends of the specimens were scarified in order to remove more dense and nontypical fatty spots of asphaltic mixture that sometimes occur during compaction.

Voids were calculated by water permeability obtained during a vacuum saturation process after the specimens were coated, scarified, and weighed. Each specimen was placed in a dry glass jar, and a vacuum of 4 in. of mercury was applied for 30 min. Distilled water was introduced into the jar, and all remained at the vacuum for a second 30 min. The jar and its contents were then released from the vacuum to atmospheric pressure and allowed to stand a minimum of 30 min. The water was always at a 2-in. minimum above the top of the specimen in the jar during the second and third 30-min steps. Distilled water was used. Specimens were weighed for calculating permeable voids prior to permeability testing. This was the standard vacuum saturation procedure for all specimens tested in thermal cycling as well.

After saturation, specimens were placed in a rubber boot. Attached to the bottom of the boot was a plate with inlet connected to the water supply from the falling head tube. Two uniform tension straps secured the top of the boot to the specimen. Usually $1\frac{1}{2}$ ft of water in the 2-in. diameter falling tube were allowed to pass through each specimen before it was refilled and the test measurements started. Tests were run at room temperature, and distilled water was used. Specimens were weighed after permeability testing. Usually a gain or loss of 2 to 3 grams of pore water was noted.

A special study of asphaltic mixture permeability would require apparatus more conducive to the determination of the coefficient of permeability. A test setup including a back pressure saturator as reported by Vallerga (11) would be a method for achieving accurate coefficients of permeability by using a minimum number of specimens.

Coefficients of permeability were plotted versus mixture voids. The coefficients increased as voids increased: 5×10^{-5} cm/sec at 4.7 percent voids, 10×10^{-5} cm/sec at 5.5 percent voids, 20×10^{-5} cm/sec at 6.5 percent voids, 100×10^{-5} cm/sec at 7.5 percent voids, and $1{,}000 \times 10^{-5}$ cm/sec at 8.5 percent voids.

It was very difficult to obtain permeable voids for the mixtures much lower than 4.5 percent by using the laboratory-compaction apparatus (kneading compactor) without crushing the aggregate and without adding more asphalt than what was reported as design content. Consequently, a 4 to 5 percent void range may be the lowest encountered for these mixtures on the road. Field results show this to be true. One, therefore, can conclude that all 3 mixtures are permeable to water and could be saturated at some or all of the time while in service.

Wetted Surface Area

If the wetted surface area of the specimen's voids is considered, it is possible to use the coefficient of permeability and porosity (voids, percent/100) to calculate this

wetted area. This wetted area may be significant in the mechanism of stripping or other failure under the influence of water.

The basic derivation of wetted surface area can be found in permeability sections of some soil mechanics books. We used the derivation of the Kozeny-Carman relationship as presented by Young and Warkentin (12).

The relationship is

$$k = \frac{C_S}{nT^2S^2} \times \frac{n^3}{(1-n)^2}$$

where

k = coefficient of permeability, cm/sec;
C_S = pore shape factor (assumed to be 0.4);
γ = density of water, dyne/cm^3;
η = viscosity of water, poise;
T = tortuosity of pores (assumed to be $\sqrt{2}$);
S = wetted surface area per solid volume, cm^2/cm^3; and
n = porosity

For asphaltic concrete specimens, let

$$S = Aw/vs$$

where

Aw = wetted surface area or surface area of permeable voids, cm^2; and
Vs = volume of aggregate plus asphalt, cm^3.

Because n = Vv/V and V_S + Vv = V, where Vv = volume of voids, cm^3, and V = total volume, cm^3, the relationship then becomes

$$K = (Cs/T^2)(\gamma/\eta)(V/Aw)^2n^3 \quad (1)$$

If we use constants of C_S = 0.4, T = $\sqrt{2}$, and γ = 980 dyne/cm^3 and $\eta = 8.9 \times 10^{-3}$ poises, a rearrangement gives

$$Aw/V = 1.48 \times 10^2(n^3/k) \quad (2)$$

Assuming that the basic derivation and assumptions of the Kozeny-Carman relationship are valid for permeability testing of asphaltic mixture specimens, then we can calculate the wetted surface area per unit volume of specimen from void and coefficient of permeability data. It is interesting to note that both voids and coefficient of permeability are required for the calculation.

There can exist certain unlimited combinations of n and k in Eq. 2 such that Aw/V will be a constant. In other words, as voids change the coefficient of permeability could change such that the overall effect produces a constant wetted surface area within the specimen. This, however, would be unusual over a wide range in voids, considering that the aggregate-asphalt arrangement is changed during changes in compaction.

Equation 2 shows in the limits that (a) as n → 1, the mixture is essentially an open tube and the wetted surface area approaches the surface area of a specimen (4 in. diameter by 5 in. high) and equals approximately 0.40 cm^2/cm^3, and that (b) as n becomes very small, k also becomes very small and must exist if n exists as determined by vacuum saturation. In the comparison of n^3/k, the quantity then must approach zero as n approaches zero. Thus, Aw/V approaches zero.

The wetted surface area per volume, Aw/V, reaches a maximum for n (or voids) between n = 0 and n = 1. The actual n at maximum Aw/V is dependent on the characteristics of the asphaltic mixture and its compaction. The practicality of having an n less than the n corresponding to maximum Aw/V is not ascertained; however, theoretically if one compacts a mixture giving a small n below the critical value, then the wetted

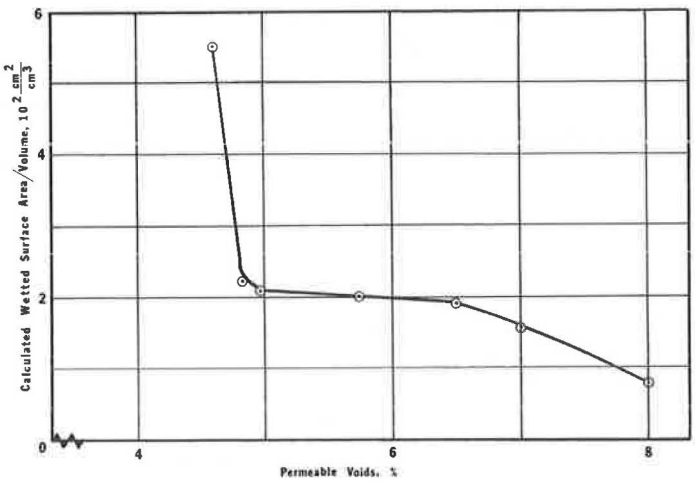

Figure 9. Wetted surface area versus voids.

surface area decreases because of pores closing up. This would be beneficial to the reduction of long-term stripping of asphalt from the aggregate. This critical value seems to occur around 3 percent voids.

Equation 2 generally is interpreted in the range of 3 to 10 percent voids. One can assume that, as voids increase for a given mixture, k will increase at a rate fast enough to make $(n^3/k)^{1/2}$ decrease. Thus, the wetted surface area should decrease. Although specimens at the higher voids will contain more quantity of water, the pore spaces are larger and provide less restricted flow. Several of the smaller pore paths combine to larger diameter paths that reduce the wetted surface area.

The wetted surface areas calculated from Eq. 2 are shown in Figure 9 as a function of voids. Aw/V data used in method 1 previously mentioned are obtained from this figure.

Interfacial Behavior of Asphaltenes

PAUL D. CRATIN, University of Miami, Coral Gables, Florida

Asphaltenes are one of many naturally occurring materials whose chemical makeup is so ill defined that classical analytical methods used to elucidate their structure, mechanism, and activity are only partly successful. Fortunately, however, data derived from measurements of their interfacial tension as a function of pH have been employed to explain and to predict their behavior with a high degree of accuracy. Based on a general technique developed by the author, a mathematical model utilizing simple chemical reactions and equilibria has been constructed that will give quantiatively (a) the relative activities of all chemical species that result from reactions of asphaltenes with hydronium and hydroxyl ions; (b) the apparent equilibrium constants that describe these reactions occurring at the oil-water interface; (c) the fraction of each of these species present as a function of pH; (d) the effect of oxygen on the chemical nature and behavior of asphaltenes; and, (e) a foundation for a mathematical criterion for emulsion stability.

•MOST natural products have a chemical makeup so ill defined that classical analytical methods used to elucidate structure, mechanism, and activity are, at best, only partially successful. Fortunately, however, data that can be obtained from straightforward surface chemical measurements may frequently be employed to explain and to predict the behavior of many complex substances, the most notable examples being naturally occurring materials whose properties depend on pH. In recent publications, Cratin and co-workers (1, 2, 3, 4) have described the development of a general method to characterize quantitatively pH-dependent systems. This technique has been used to account for such diverse phenomena as stability of crude oil emulsions, transience of some natural products, and even the specificity of enzymatic reactions. Indeed, this general method can be used for any system whose "activity" may be determined as a function of pH. (By "activity" is meant some pH-dependent property that may be in nature and is either thermodynamic, e.g., surface and interfacial free energies, or kinetic, e.g., rates of chemical reactions.)

Having established this activity-pH relationship, one can construct a mathematical model, based on simple chemical reactions and equilibria, that will give quantitatively (a) the relative activities of all chemical species that result from reactions with hydronium and hydroxyl ions; (b) the degree to which any (or all) of these species may interact; (c) the apparent equilibrium constants that describe the reactions occurring in solution or at an interface; and (d) the fraction of each species present as a function of pH.

In this paper, the general method will be used to describe the interfacial behavior of a class of highly complex, chemically ill-defined materials, the asphaltenes. Furthermore, it will be demonstrated that correct use of the method allows one to account quantitatively for the effect of oxygen on the chemical nature and behavior of asphaltenes; and finally, it will be shown that this method serves as a foundation for a mathematical criterion for emulsion stability.

Paper sponsored by Committee on Effects of Natural Elements and Chemicals on Bitumen Aggregate Combinations and presented at the 49th Annual Meeting.

EXPERIMENT

The separation of the asphaltenes from crude oils was carried out according to the method outlined by Sachanen (5). To preserve anaerobic conditions, separations were carried out in an atmosphere of dry nitrogen, and the samples were stored away from light in airtight weighing bottles. Each solvent was sparged with dry nitrogen prior to use to remove any traces of dissolved oxygen.

A stock solution of asphaltenes was prepared by extracting approximately 5 grams of the solid with 500 ml of a hot cyclohexane-benzene mixture. When cool, the resulting solution was filtered through coarse Whatman paper into a stoppered volumetric flask. This solution was kept blanketed with a dry nitrogen atmosphere. Aqueous phases were prepared by adjustment of the pH (as determined by a Beckman pH meter, model G, of triply distilled water to desired values with 0.5 N NaOH and HCl.

Interfacial tension measurements were made with a Cenco-du Nouy tensiometer fitted with a Call ring alignment joint according to the standard procedure given, for example, in Daniels (6). Added by buret into a 100-ml beaker were 35 ml of the aqueous phase, and the du Nouy ring was immersed to ensure complete wetting. Then, 25 ml of the stock asphaltene solution were carefully discharged from a pipette on to the surfaces of the aqueous phase. (Great care was exercised to avoid turbulence; at extreme pH values, turbulence would result in the formation of emulsions and the disappearance of the interface. When this occurred, the samples were discarded.) The du Nouy ring was then raised to the interface, allowed to age for 5 min, and finally pulled up through the interfacial region. The interfacial tension was determined from a corrected dial reading.

RESULTS AND DISCUSSION

Relative Interfacial Tension versus pH

The experimentally determined values for the relative interfacial tension as a function of pH are shown in Figure 1. (For reasons that will become obvious later, interfacial tensions are expressed on a relative rather than on an absolute scale.)

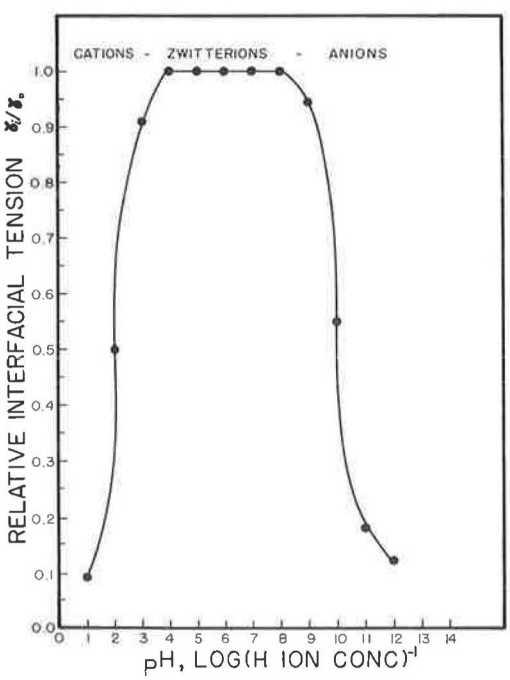

Figure 1. Experimental relative interfacial tension as function of pH (anaerobic).

A great deal of information can be gleaned from the general shape of the γ_i/γ_0 versus pH curve. The fact that the interfacial tension is high in the intermediate pH region (i.e., 4 to 8) and that it falls off rapidly in both acidic and basic solutions indicates that asphaltenes are amphoteric in nature. That this is true may be shown by the following argument.

Their large degree of aromaticity and their enormous molecular weights render the asphaltenes virtually insoluble in water but somewhat soluble in organic liquids. If basic groups on the asphaltene "molecule" were present, they would be protonated at low pH values to species that, being ionic, would show some hydrophilic character. The tendency of the hydrophilic "part of the molecule" to migrate into the aqueous phase would be partially offset by the driving force of the hydrophobic "part of the molecule" to remain in the organic phase. The result would be a concentration

buildup at the oil-water interface, thus causing a lowering of the interfacial tension—a phenomenon that is observed experimentally. This argument can be extended for regions of high pH where the asphaltenes would react with hydroxyl ions to form anionic "soaps," materials that also possess a remarkable ability to lower the interfacial tension. If this argument is valid, one can postulate the existence of a charge-neutral species (hereafter referred to as the "zwitterion") in the region of the broad, flat maximum shown in Figure 1. At low pH values, the dominant species is a positively charged moiety that we shall call the cationic species (cations). In regions of high pH, the species of greatest concentrations is a negatively charged "molecule" that we shall refer to as the anionic species (anions). Between the extreme values of γ_i/γ_0 in the region of low pH, there exists a mixed interfacial film that consists of zwitterions and cations. In the higher pH region, the interfacial film is composed of zwitterions and anions.

Mathematical Model Proposed

In order to visualize what appears to happen at the molecular level, let us suppose we have our system initially in a region of very low pH. Virtually all of the asphaltene material will have been converted to the cationic species that we shall abbreviate as HZ^+. If we now add small quantities of a base, say, a solution of NaOH, there ensues a chemical reaction that is described by

$$HZ^+ + OH^- = Z^{\pm} + H_2O \tag{1}$$

where $Z^{\pm}$ is the zwitterion.

An apparent equilibrium constant for this reaction may be written as follows:

$$K_b = \frac{(HZ^+)(OH^-)}{(Z^{\pm})} \tag{2}$$

Let us now suppose we have our system in a region of very high pH where the predominant species is the anion, Z^-. Addition of small quantities of an acid, for example, a solution of HCl, will cause the following reaction to occur:

$$Z^- + H^+ = Z^{\pm} \tag{3}$$

The apparent equilibrium constant associated with this chemical reaction is

$$K_a = \frac{(H^+)(Z^-)}{(Z^{\pm})} \tag{4}$$

It is obvious that the total concentration of material at the oil-water interface, $(Z)_t$, is given by the sum of all the species present, i.e.,

$$(Z)_t = (Z^{\pm}) + (HZ^+) + (Z^-) \tag{5}$$

It should also be obvious that the terms on the right side of Eq. 5 are themselves not independent but are related quantitatively to one another through Eqs. 1 through 4.

It appears at first glance that we are faced with an insurmountable problem: The chemical nature of pitch and its derivatives are extremely ill defined, and no interfacial concentration can be measured experimentally. This problem can be eliminated, fortunately, by expressing all concentrations in terms of (mole) fractions. For example, the fraction of zwitterion, $f_{\pm}$, is defined by

$$f_{\pm} \equiv \frac{(Z^{\pm})}{(Z)_t} \tag{6}$$

The following example is given to illustrate how analytical expressions describing the relationships between fraction and pH may be derived (Fig. 2).

$$(Z^{\pm}) = (Z^{\pm}) \tag{7}$$

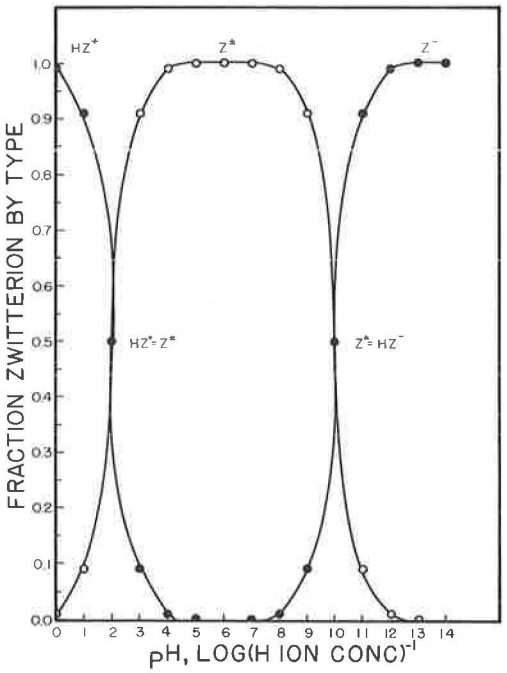

Figure 2. Fractions of cationic (HZ^+), zwitterionic ($Z^{\pm}$), and anionic species as functions of pH.

From Eq. 2

$$(HZ^+) = \frac{K_b(Z^{\pm})}{(OH^-)} \tag{8}$$

and from Eq. 4

$$(Z^-) = \frac{K_a(Z^{\pm})}{(H^+)} \tag{9}$$

Adding Eqs. 7, 8, and 9 and substituting into Eq. 5, we obtain

$$(Z)_t = (Z^{\pm})\left[1 + \frac{K_b}{(OH^-)} + \frac{K_a}{(H^+)}\right] \tag{10}$$

There exists another relationship in water and in aqueous solutions that we shall use to eliminate another variable, (OH^-), i.e.,

$$(H^+)(OH^-) = K_w \tag{11}$$

Substituting $K_w/(H^+)$ for (OH^-) in Eq. 10, we find that

$$(Z)_t = (Z^{\pm})\left[1 + \frac{K_b(H^+)}{K_w} + \frac{K_a}{(H^+)}\right] \tag{12}$$

Equation 12 is now rearranged to a somewhat different form:

$$\frac{(Z^{\pm})}{(Z)_t} \equiv f_{\pm} = \frac{(H^+)K_w}{(H^+)^2K_b + (H^+)K_w + K_aK_w} \tag{13}$$

Likewise, expressions for the cationic (f_+) and anionic (f_-) species may be derived as follows:

$$f_+ = \frac{(H^+)^2K_b}{(H^+)^2K_b + (H^+)K_w + K_aK_w} \tag{14}$$

and

$$f_- = \frac{K_aK_w}{(H^+)^2K_b + (H^+)K_w + K_aK_w} \tag{15}$$

To characterize the composition of the interface over the entire pH range requires a knowledge of the values of K_a and K_b. In their original study, Cratin and Dean (2) reasoned as follows:

> Aware that the amphoteric asphaltenes are quite similar to the amino acids, we constructed a plot of $f^{\pm}$ versus pH for glycine. The curve obtained was identical in shape to that in Figure 1. Upon further analysis, it was found that, in the case of glycine the inflection point in the left hand leg occurred when $(Z^{\pm}) = (HZ^+)$, that is, at half-neutralization, so that pH = 14 - pK_b. On the right hand side, the inflection point corresponded to the condition $(Z^{\pm}) = (Z^-)$ (again at half-neutralization), so that pH = pK_a. The maximum in the glycine curve occurred at the isoelectric point, i.e., where

$$(H^+) = \sqrt{KaKw/K_b}$$

To complete the argument, we reasoned that the interfacial tensions of the asphaltenes are directly related to the fraction of zwitterion present. Thus, $f_\pm$ will be a maximum at the charge-neutralization (i.e., isoelectric) point; since the interfacial activity will be a minimum here, the interfacial tension will be at its maximum value. The decrease in $f_\pm$ is accompanied by an increase in f_+ or f_-, depending upon pH, and since these materials are more interfacially active than $Z^\pm$, the interfacial tension will accordingly decrease.

It is now possible to use Figure 1 to determine the pH values at which equimolar mixtures of the zwitterion and the charged species co-exist at the interface. From the pH values taken at the two points of inflection K_a and K_b were calculated with the equations: $pK_b = 14 - pH$ (left-hand side) and $pK_a = pH$ (right-hand side). The values of K_a and K_b were found to be: $K_a = 10^{-10}$ and $K_b = 10^{-12}$. A compilation of the fraction of each species as a function of the pH is given in Table 1.

As a consequence of this analysis, there now exists a method to determine whether these species which co-exist at the interface do so independently or do so antagonistically. If they co-exist independently, then the activities of the species will remain constant throughout the pH range over which they are present. Should they exhibit an antagonistic effect, this will be reflected in the inconstancy of their activities.

Successful completion of the argument requires a suitable definition of the interfacial activity, Φ. This variable must be readily calculated from experimental measurements, and its values must have real significance. Cratin and Dean (2) proposed a definition based on the relative lowering of the interfacial activity.

$$\Phi \equiv \frac{\gamma_0 - \gamma_i}{\gamma_0} \tag{16}$$

where γ_0 is the highest interfacial tension exhibited by the system throughout the pH range, and γ_i is the interfacial tension observed under the conditions for which Φ is calculated. This definition is most useful, for not only does it relate to experimentally determinable properties but also it places logical limits on its values. To illustrate this, let us consider a substance (such as a detergent) capable of reducing the interfacial tension to zero. This is equivalent to saying that this substance possesses the maximum degree of activity, i.e., $\Phi = 1$. Conversely, a substance that does not affect the interfacial tension is said to have no degree of activity. Mathematically, $\gamma_i = \gamma_0$, and $\Phi = 0$.

Having chosen a definition for interfacial activity, we must now demonstrate how this will provide information about independent (or not) coexistence. If the various species coexist independently, the total activity will be equal to the sum of the contributions from all species. That is to say,

$$\Phi = \frac{\gamma_0 - \gamma_i}{\gamma_0} = \sum_i \phi_i f_i \tag{17}$$

$$\frac{\gamma_i}{\gamma_0} = 1 - (\phi_\pm f_\pm + \phi_+ f_+ + \phi_- f_-) \tag{18}$$

The working equation from which a (γ_i/γ_0) versus pH curve is constructed is obtained by substitution of Eqs. 13, 14, and 15 into Eq. 18. The final result is as follows (the reason for plotting the relative interfacial tension in Figure 1 now becomes apparent):

$$\frac{\gamma_i}{\gamma_0} = 1 - \left[\frac{\phi_\pm (H^+) K_w + \phi_+ (H^+)^2 K_b + \phi - K_a K_w}{(H^+)^2 K_b + (H^+) K_w + K_a K_w}\right] \tag{19}$$

TABLE 1

$f_{\pm}$, f_+, AND f_- AS FUNCTION OF pH

pH	$f_{\pm}$	f_+	f_-	pH	$f_{\pm}$	f_+	f_-
0	0.01	0.99	10^{-10}	8	0.99	10^{-6}	0.01
1	0.09	0.91	10^{-9}	9	0.91	10^{-7}	0.09
2	0.5	0.5	10^{-8}	10	0.50	10^{-8}	0.50
3	0.91	0.09	10^{-7}	11	0.09	10^{-10}	0.91
4	0.99	0.01	10^{-6}	12	0.01	10^{-12}	0.99
5	0.99+	10^{-3}	10^{-5}	13	10^{-3}	10^{-14}	0.99+
6	0.99+	10^{-4}	10^{-4}	14	10^{-4}	10^{-16}	0.99+
7	0.99+	10^{-5}	10^{-3}				

Note: $K_a = 10^{-10}$, and $K_b = 10^{-12}$.

Equation 19 contains 3 variables yet to be determined: $\phi_{\pm}$, ϕ_+, and ϕ_-. These can be found in the following manner:

1. At pH = 6, nearly all the asphaltenes are in the zwitterionic form. (The fractions of cationic and anionic species are about 10^{-4}.) Hence, as a first approximation, we shall let $f_+ = f_- =$ zero, and $f_{\pm} = 1$. Substituting these values into Eq. 19, we obtain

$$\frac{\gamma_i}{\gamma_0} \rightarrow 1 - \phi_{\pm} \qquad (20)$$

Because $\gamma_i = \gamma_0$ and $\frac{\gamma_i}{\gamma_0} = 1$ at pH = 6, $\phi_{\pm}$ is found to be zero.

2. At pH = 10, $f_+ = 10^{-8}$, $f_- = f_{\pm} = 0.5$, and $(\gamma_i/\gamma_0) = 0.55$; ϕ_- then is 0.90.
3. At pH = 2, $f_- = 10^{-8}$, $f_+ = f_{\pm} = 0.5$, and $(\gamma_i/\gamma_0) = 0.50$; ϕ_+ is found to be 1.00.

In its final form, Eq. 19 becomes

$$\frac{\gamma_i}{\gamma_0} = 1 - \left[\frac{(H^+)^2 K_b + 0.90\, K_a K_w}{(H^+)^2 K_b + (H^+) K_w + K_a K_w}\right] \qquad (21)$$

(Recall that these values were obtained by Cratin and Dean's "eyeball" method. Recently, a computer analysis of their data gave the "best values" for K_a and K_b as 9.43×10^{-11} and 9.97×10^{-13} respectively.) The values given in Table 2 were calculated from Eq. 21. A graphical comparison of the theoretical values with experimental data is shown in Figure 3.

Interpretation

The near-perfect agreement between theory and experiment, which extends for 14 orders of magnitude in hydrogen ion concentration, strongly attests to the validity of the model and the assumptions. It is clear that Eq. 21 describes the interfacial behavior of this system very well; and, furthermore, one can state that as-

TABLE 2

CALCULATED AND EXPERIMENTAL VALUES OF γ_i/γ_0 AS FUNCTION OF pH

pH	Calculated γ_i/γ_0	Experimental γ_i/γ_0	pH	Calculated γ_i/γ_0	Experimental γ_i/γ_0
0	0.01	—	8	0.99	1
1	0.09	0.09	9	0.91	0.97
2	0.50	0.50	10	0.55	0.55
3	0.91	0.91	11	0.18	0.18
4	0.99	1	12	0.10	0.12
5	0.99+	1	13	0.10	—
6	0.99+	1	14	0.10	—
7	0.99+	1			

Note: $\phi_{\pm} = 0.00$; $\phi_+ = 1.00$; $\phi_- = 0.90$; $K_a = 10^{-10}$; $K_b = 10^{-12}$; and $\gamma_0 = 21.0$ dynes cm^{-1}.

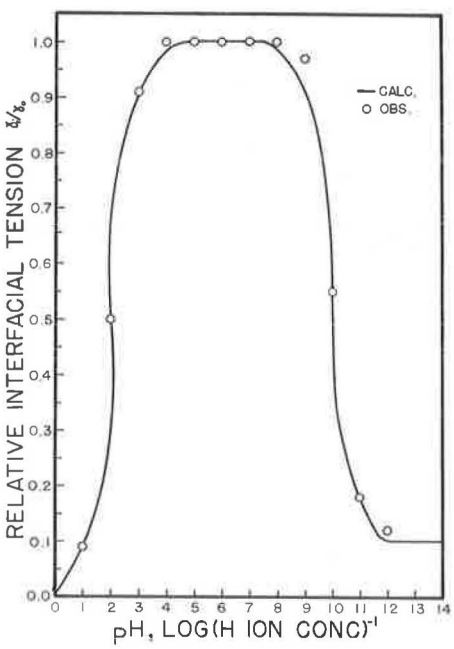

Figure 3. Comparison of experimental and calculated relative interfacial tensions as functions of pH anaerobic).

phaltenes and their derivatives coexist independently at the oil-water interface over the entire pH range. Evidence for any molecular interactions is completely lacking.

Emulsion Stability and pH

The broad maximum shown in Figure 1 occurs in the pH range where water-in-oil emulsion stability is greatest because of the formation of rigid interfacial films. Likewise, it corresponds to the region where the predominant species is the zwitterion. As the pH is changed (raised or lowered), the interfacial tension undergoes a rapid drop to near zero, a value that is necessary for the stabilization of oil-in-water emulsions. These emulsions are stabilized not by rigid films but by "mobile," or surfactant, films (7, 8). In the transition from rigid to surfactant films, the system passes through a phase-inversion point, that is, a region where a water-in-oil emulsion inverts to become an oil-in-water type. Hence, it is at the phase-inversion point that emulsion stability will be at a minimum. Before the phase-inversion point is reached, the great majority of surfactants present at the interface are those tending to stabilize water-in-oil emulsions by the formation of rigid films. Beyond the phase-inversion point, the greater number of surfactant molecules present are those that tend to stabilize oil-in-water emulsions through electrical effects and a low interfacial tension. It is reasonable to assume that regions of instability will occur when approximately equal numbers of surfactants coexist at the oil-water interface—one type tending to stabilize water-in-oil emulsions and the other trying to stabilize the oil-in-water type. These regions of instability correspond precisely to the points of inflection in the γ_i/γ_0 versus pH curve. Below the isoelectric point, minimum stability exists when $(HZ^+) = (Z^\pm)$; above, the isoelectric point minimum stability occurs when $(Z^-) = (Z^\pm)$.

A stability-pH profile has recently been proposed by Cratin (9). He defined a stability index, S, for a system containing 2 surfactant species as

$$S \equiv 1 - 2f_i f_j \qquad (22)$$

where f_i and f_j are fractions of the respective surfactant species present in the interface.

Table 3 gives a compilation of data calculated by using the fractions (Table 1) and Eq. 22. A plot of S versus pH is shown in Figure 4. An inspection of Figure 4 shows that there are 3 regions of high stability: (a) at low pH values where oil-in-water emulsions are favored because of the presence of positively charged, i.e., cationic, surfactants; (b) at high pH values where oil-in-water emulsions are also favored because the surfactants are nega-

TABLE 3

EMULSION STABILITY INDEX AS FUNCTION OF pH

pH	$f_+ f_\pm$	$f_\pm f_-$	S	pH	$f_+ f_\pm$	$f_\pm f_-$	S
0	0.01	10^{-12}	0.98	8	10^{-6}	0.01	0.98
1	0.08	10^{-10}	0.84	9	10^{-7}	0.08	0.84
2	0.25	10^{-9}	0.50	10	10^{-9}	0.25	0.50
3	0.08	10^{-7}	0.84	11	10^{-11}	0.08	0.84
4	0.01	10^{-6}	0.98	12	10^{-14}	0.01	0.98
5	10^{-3}	10^{-5}	1	13	10^{-17}	10^{-3}	1
6	10^{-4}	10^{-4}	1	14	10^{-20}	10^{-4}	1
7	10^{-5}	10^{-3}	1				

Note: $K_a = 10^{-10}$, and $K_b = 10^{-12}$.

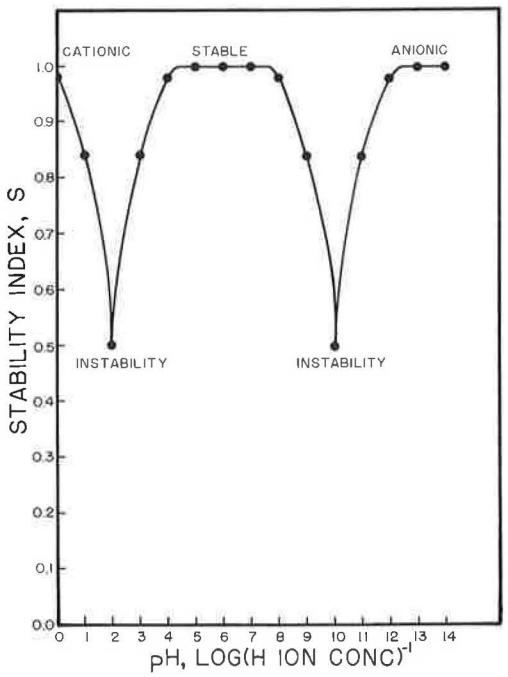

Figure 4. Emulsion stability index as function of pH.

tively charged, i.e., anionic; and (c) at intermediate pH values where water-in-oil emulsions are stable because of the presence of uncharged, i.e., zwitterionic species that offer stability through the formation of rigid films. Likewise, Eq. 22 predicts 2 points of minimum stability: at pH = 2 where $(HZ^+) = (Z^\pm)$, and at pH = 10 where $(Z^-) = (Z^\pm)$. These predictions have been confirmed experimentally.

Effect of Oxygen on Asphaltene Behavior

Several interesting observations were made on systems from which air had not been excluded during separation and purification of the asphaltenes. Figure 5 shows the relative interfacial tension as a function of pH under nonanaerobic conditions. The left side of the curve has become truncated to such an extent that it is almost nonexistent, while the right side has changed very little aside from its dropping to near zero at high pH values. The results of a mathematical analysis of these data show that (a) the values of K_a and K_b are, within experimental error, identical to those values of K_a and K_b for the anaerobic asphaltene system; (b) the activity of the anionic species, ϕ_-, rose to 1.00; and (c) the activity of the cationic species, ϕ_+, dropped to 0.14.

These results can be interpreted in the following manner: The fact that K_a and K_b remained unchanged indicates that the types of chemical groups on the asphaltene "molecule" are probably the same for both classes of asphaltenes. The rise in ϕ_- can be attributed to the increase in the number of acid groups (which, at high pH values, are converted to active soaps) arising from the oxidation of unsaturated chemical bonds in the molecule. The fall in ϕ_+ can be ascribed to the oxidation of some basic groups to nonbasic species. Because the oxidized form cannot react with hydronium ions to become cationic, the overall interfacial activity decreases. A most significant fact is that the method tells the magnitude of the change: 86 percent of the basic groups were destroyed!

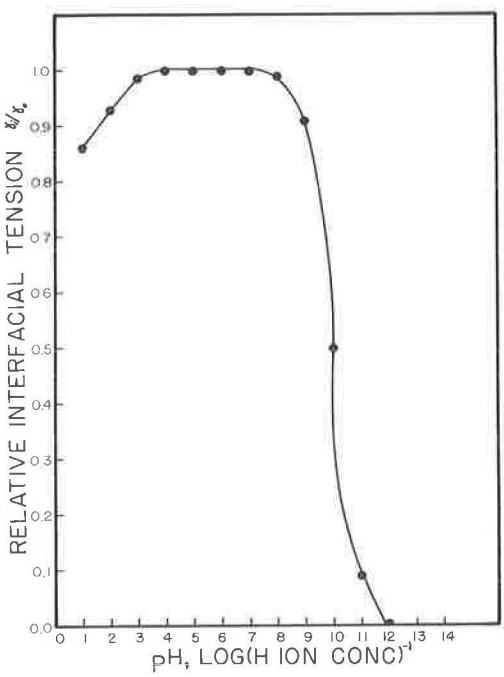

Figure 5. Experimental relative interfacial tension as function of pH (nonanaerobic).

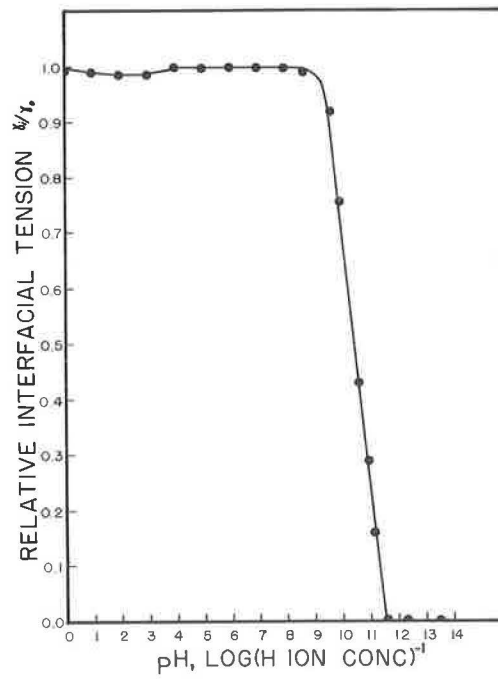

Figure 6. Experimental relative interfacial tension of stearic acid as function of pH.

If this explanation is valid, then a molecule containing only acid (no basic) groups should exhibit large relative interfacial tensions until a region of high pH is reached. To check this, Cratin and Zetlmeisl (10) measured the interfacial tension of a solution of stearic acid as a function of pH. Their findings, as shown in Figure 6, offer unequivocal support for the validity of this explanation.

CONCLUSION

The research described in this paper is but a single example of how this general method, when properly used, can characterize quantitatively any system whose properties are sensitive to pH. Indeed, the phenomenal amount of information that has been gleaned from these experimental data serves to emphasize the utility of this general method and points to its future use to explain the behavior of many such ill-defined systems.

REFERENCES

1. Cratin, P. D. A Quantitative Characterization of pH-Dependent Systems. Ind. and Eng. Chem., Vol. 61, No. 2, 1969, p. 35.
2. Cratin, P. D., and Dean, A. M. Interfacial Activities of Crude Oil Surfactants: A Mathematical Approach to Mixed Films. Jour. Alabama Acad. Sci., Vol. 37, 1966, p. 228.
3. Cratin, P. D., and Murray, J. M. A Quantitative Surface Chemical Characterization of Pitch. Paper submitted for publication.
4. Murray, J. M. A Mathematical Model of Enzymatic Behavior. Jour. Alabama Acad. Sci., Vol. 39, No. 2, 1968, p. 110.
5. Sachanen, A. N. The Chemical Constituents of Petroleum. Reinhold Publishing Corp., New York, 1945, pp. 385-413.
6. Daniels, F., et al. Experimental Physical Chemistry. McGraw-Hill, New York, 1956, pp. 51-60.
7. Schulman, J. H., and Cockbain, E. G. Molecular Interactions at Oil-Water Interfaces: Part I—Molecular Complex Formation and the Stability of Oil-in-Water Emulsions. Trans. Faraday Soc., Vol. 36, 1940, pp. 651-660.
8. Schulman, J. H., and Cockbain, E. G. Molecular Interactions at Oil-Water Interfaces: Part II—Phase Inversion and Stability of Water-in-Oil Emulsions. Trans. Faraday Soc., Vol. 36, 1940, pp. 661-668.
9. Cratin, P. D. A Mathematical Stability Index for Emulsions. Jour. Alabama Acad. Sci., Vol. 38, No. 4, 1967, p. 336.
10. Cratin, P. D., and Zetlmeisl, M. J. Unpublished work done at Spring Hill College, Mobile, Ala., 1966.

An Investigation of Asphalt-Aggregate Adhesion by Measurements of Heats of Immersion

E. KEITH ENSLEY, U.S. Bureau of Mines, Laramie, Wyoming; and
HENRY A. SCHOLZ, Kennecott Copper, Ely, Nevada

This paper discusses the problems in studying asphalt-aggregate adhesion and the relation between adhesion and heats of immersion. The construction of a microcalorimeter and its application in measuring the energy of interaction between road asphalts and aggregates are described. Experimental heat of immersion curves are presented on quartz, calcite, a phosphate slag, and 4 Montana aggregates used with a commercial asphalt. The effect of an antistripping agent on heats of immersion was evaluated.

•THEORETICAL calculations of the microscopic properties at the asphalt-aggregate interface will probably remain impossible to perform for asphalt-aggregate interactions. Such a statement is secured by the variances and complexities of asphalts and surfaces of aggregates. Asphalt researchers have, therefore, had to rely on empirical and semi-empirical approaches to their problems. Examples of purely empirical approaches to asphalt-aggregate adhesion are peeling, scraping, and stripping techniques (1, 2, 3). Although such disciplines may not excite the pure scientist, they nevertheless have been useful in evaluating asphalt-aggregate interactions. The methods are not free of problems. Often the percentage of asphalt adhering to the aggregate surface is determined by unreliable visual observation. Another problem is surface roughness that leads to spurious results.

Semi-empirical approaches to asphalt-aggregate adhesion include contact angle (1) and sessile drop (2) studies. Again surface variations impair reproducibility. Also, the contact angle studies do not allow accurate measurements, because the angle is too small and they are further plagued with a hysteresis effect.

These approaches have been mentioned to point out the need for a reliable method for studying asphalt-aggregate interactions. With such a purpose as a goal, a thermodynamic approach through the study of heat of immersion was pursued.

The heat of immersion is the energy released when an insoluble solid is dropped into a liquid. The energy is proportional to the adhesion or interfacial bond between the liquid and the solid surface. It is highly probable that for a given adsorbent and adsorbate the bond strength will vary over the surfaces. For example, molecules adsorbed in a crevice will be bonded stronger than those on the edge or on flat surfaces. Also, heterogeneity is certain to be present because of Schottky and Frenkel defects or dislocations. Naturally occurring aggregates or minerals would add another variable, heterogeneous chemical composition.

Zettlemoyer (6) sums up the various contributions to immersional energy by stating that the heat liberated will be determined by "...the average polarity of solid surfaces, site energy distribution or heterogeneity of solid surfaces, solution adsorption, ...and heat of formation of double layers."

Because of the complex nature of the aggregate surfaces, as well as the complexities of the asphalt, we cannot attribute immersional energy to any one type of bond. Rather we can expect several types of bonds to be present because of forces such as ionic, permanent dipole, induced dipole, and dispersion. Regardless of which forces

Paper sponsored by Committee on Effects of Natural Elements and Chemicals on Bitumen Aggregate Combinations and presented at the 49th Annual Meeting.

are present, it should be reasonable to assume that the greater the energy that is released in the immersional process, the stronger will be the asphalt-aggregate bond. We can extend this postulate by stating that the stronger the bond the better will be the performance of the asphalt in the road.

EXPERIMENTAL SECTION

The energy released in the heat of immersion is always small and requires a very sensitive calorimeter for detection. To measure the energy released in the asphalt-aggregate interaction, a differential microcalorimeter (7) of the Tian-Calvet type was constructed.

Construction of the Microcalorimeter

The thermopile assembly consists of 1,200 electroplated copper-constantan thermocouples. Earlier works discuss electroplated thermocouples (8, 9) and the application to microcalorimetery (10). The assembly contains 40 mica disks or wafers ($^3/_8$-in. inner diameter and $2^1/_4$-in. outer diameter), each wrapped 30 times with constantan wire. One side of each disk was electroplated with copper while the opposite side was masked. (The electroplated junctions are 50 percent as efficient was welded junctions.) The wafers are stacked around the cell holder (Fig. 1, E) and sandwiched between small anodized aluminum rings (Fig. 1, C), large anodized aluminum rings (Fig. 1, B), and additional mica wafers to eliminate shorting between wire-wrapped wafers. Two similar thermopile assemblies were constructed and connected in opposition as in differential thermal analysis. The signal from the differential thermopile is fed into a Keithley 149 millimicro-voltmeter and into a recorder.

The reaction cell holder (4 in long and $^5/_8$ in. inner diameter) was anodized on the outside to eliminate shorting the junctions that were in thermal contact with the holder. The inner wall is in good thermal contact with the reaction cell containing the asphalt. A Teflon aggregate holder is clamped to the top of the reaction cell. The aggregate is held in the container by a trapdoor that is sprung by a trip wire extending to the outside of the oven. A 10.0-ohm manganin wire-wound calibrating resistor is connected to the Teflon holder and is immersed into the asphalt as the holder is connected to the reaction cell. (After each run a calibration was performed by passing a known quantity of electricity through the coil.) Small mica shelves were placed on the coil for dispersing the aggregate.

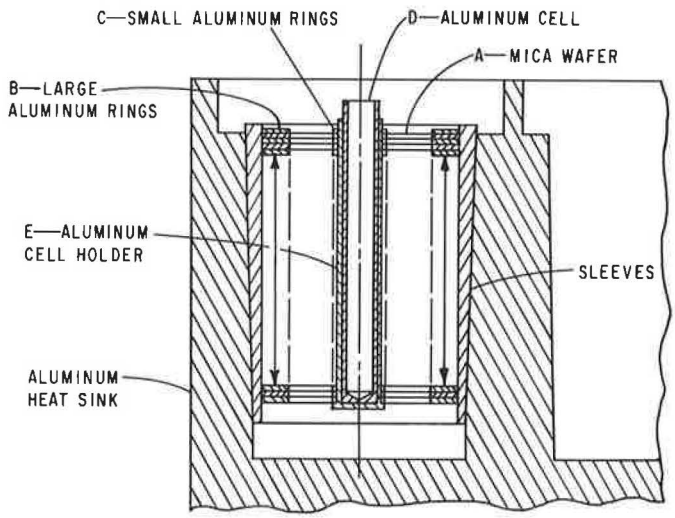

Figure 1. Cross section of the reaction cell and thermopile assembly.

The cylindrical heat sink (Fig. 1) and tapered sleeves constitute the heat sink. The sleeves are split to aid in removal of the thermopile. Thermal fluctuations within the heat sink are reduced to a minimum by a 20-lb aluminum heat-sink lid, a ½-in. thick aluminum can surrounding the microcalorimeter, and a ⅜-in. thick steel can surrounding the aluminum can.

The total assembly is enclosed in a constant temperature oven at 150 C. Three parallel heating coils are on continuously; a fourth coil is controlled by a thermistor.

Materials

Specimen-grade quartz and calcite were tested as aggregate standards. Also tested were 2 aggregates from Glacier County (differentiated by No. 2 and No. 3), one from Teton County and one from Lewis and Clark County, and a phosphate slag from Silver Bow County.

The aggregate samples were prepared by crushing, screening to obtain -35 +48 M size, and washing with distilled water. They were dried overnight at 150 C. (No difference could be detected in the heat of immersion between these samples and samples that had been dried at 400 C for 12 hours under a vacuum of 10^{-6} torr.) The surface area of the aggregates was assumed to be 149 cm^2/g, a value given by Bikerman (11) for quartz.

Only one asphalt was tested. It was an Arkansas penetration grade 36 asphalt (Bureau of Public Roads No. B-3036). The asphalt was tested both untreated and treated with 1 percent Armour Diamine-Redicote 80-S, which is a fatty acid salt of a long-chain fatty diamine.

Procedure

In a typical run, 5 g of asphalt was poured into the reaction cell. A ½-g sample of aggregate was accurately weighed in the Teflon sample holder and the calibration coil attached to the holder. Inasmuch as the holder was connected to the reaction cell, the coil was immersed into the asphalt. The reaction cell was placed in the cell holder in the reaction side of the microcalorimeter. A blank cell containing asphalt but not aggregate was placed in the other side of the microcalorimeter. After a period of 48 hours the trapdoor was sprung allowing the aggregate to drop into the asphalt.

The immersional energy produced was recorded for 3 hours or more. The curves were calibrated and replotted in $ergs/cm^2$-min versus time in minutes.

RESULTS AND DISCUSSION

The nature of the reaction between asphalt and aggregates prohibits the usual method of reporting immersional data. No finite value is obtained but rather energy is released for a long period of time. A typical example is quartz into asphalt.

The bottom curve shown in Figure 2 represents the immersion of quartz into B-3036 test asphalt at 150 C. The shape of the curve is similar to shapes of curves obtained for all aggregates, an initial peak followed by a long tail. A second curve, shown in Figure 2, represents the immersion of quartz into B-3036 asphalt containing 1 percent of the Armour amine salt. The initial peak height is doubled and the tail height is 10 times higher with the amine present. Weber (12) noted by strip tests that the amine additive does improve certain asphalt-aggregate adhesion. Based on the analysis of the strip test data, the tail height may be more representative of resistance to stripping than the initial peak height.

Calcite was selected to represent the alkaline class of rocks. The surface area was assumed to be the same as that for the quartz; however, this is recognized as only an approximation. The immersion curve for the calcite-asphalt reaction is shown in Figure 3. The initial peak is about equal to the peak height for quartz, but the tail is 6 times higher for calcite. This would indicate that, if the strip test correlation cited earlier holds, then calcite bonds better than quartz to the test asphalt. The type of material that gives the best bond is a controversial topic (13).

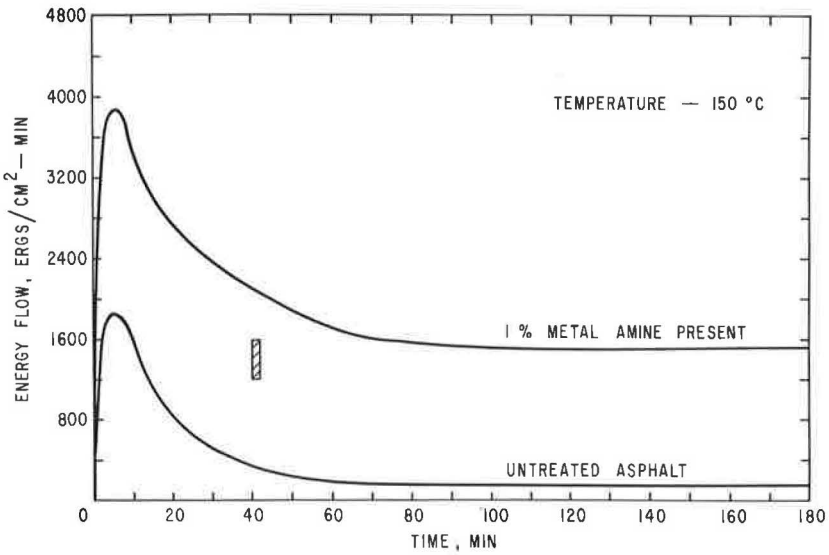

Figure 2. Heat of immersion of quartz into treated and untreated asphalt. (The shaded rectangle in this and following figures represents 800 ergs/cm^2 and is given for comparative analysis.)

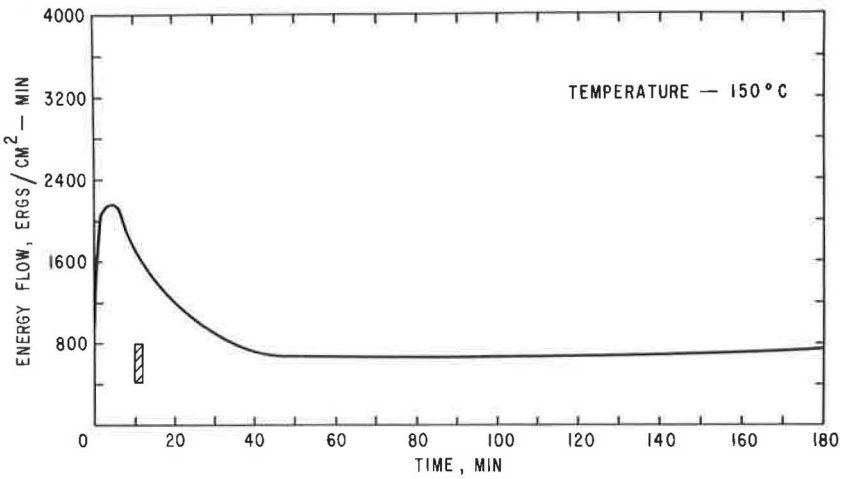

Figure 3. Heat of immersion of calcite into untreated asphalt.

A phosphate slag, which was used in highway construction near Butte, was investigated by immersion studies. Figure 4 shows 2 curves resulting from the immersion of the slag into asphalt. The bottom curve was obtained for untreated asphalt and the upper curve for the amine salt-treated asphalt. Doping produced a large increase in area under the curve. This increase is probably due to the acidic surface of the slag forming an excellent bond with the amine salt.

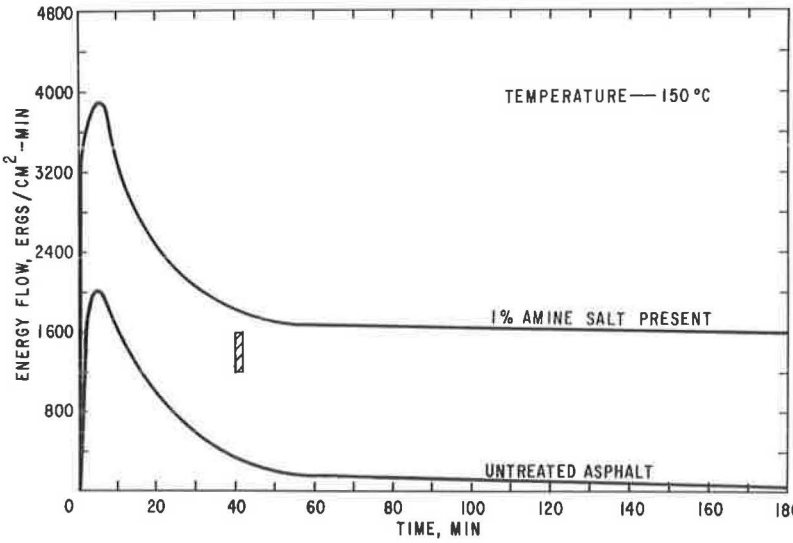

Figure 4. Heat of immersion of a phosphate slag into treated and untreated asphalt.

The aggregates from Glacier County and Lewis and Clark County were principally silicate rocks. The Teton County aggregate was limestone. The immersion curves for Teton County and Glacier County No. 3 aggregates are shown in Figure 5. They had higher curve tails but lower initial peaks than the other 2 Montana aggregates (Fig. 6). All the aggregates had higher curves than pure quartz.

The adhesion of asphalt to these 4 aggregates has been examined by Weber (12). He has shown by a strip test that Teton County and Glacier County No. 3 aggregates gave the best adhesion with asphalt and that the former being was the best of the two. His

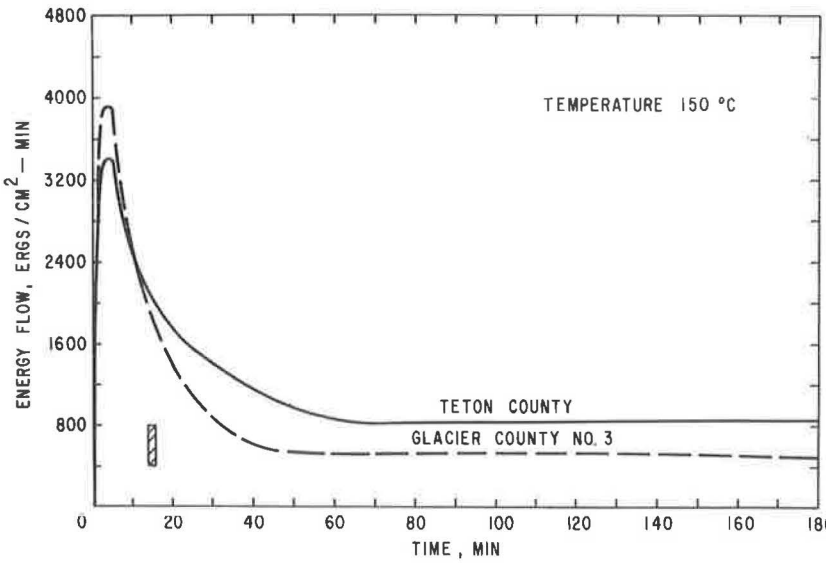

Figure 5. Heat of immersion of two Montana aggregates into asphalt.

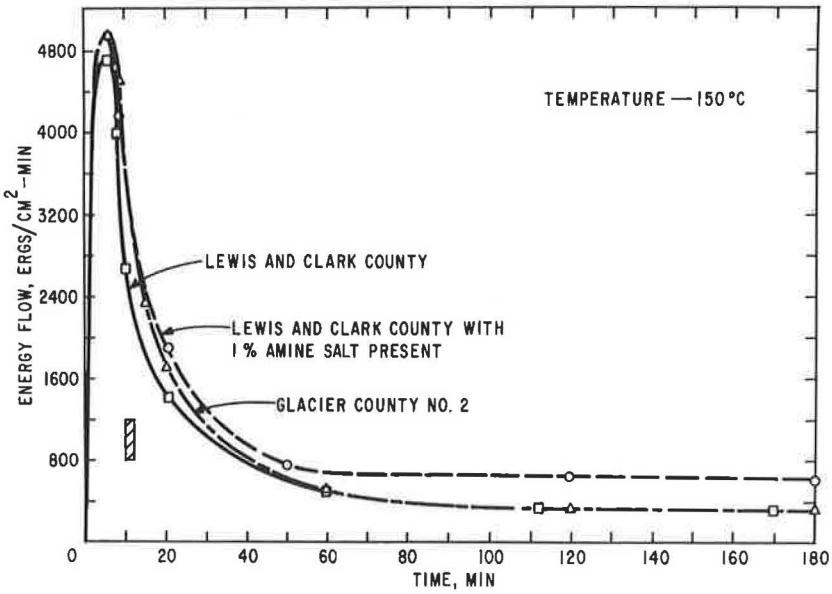

Figure 6. Heat of immersion of Glacier County No. 2 aggregate into untreated asphalt and Lewis and Clark County aggregate into both treated and untreated asphalt.

observations agree with the immersion data, assuming that greater tail heights indicate better resistance to stripping. Weber also observed that the addition of the amine salt to the asphalt improved the adhesion to Glacier County No. 2 and Lewis and Clark County aggregates. Adhesion that was poor with untreated asphalt became comparable to that observed for the Teton County and Glacier County No. 3 aggregates with the untreated asphalts. We did not detect a large difference in treated and untreated asphalts with Glacier County No. 2 aggregate, but the tail height was doubled for Lewis and Clark County aggregates (Fig. 6).

The immersional energy from asphalt-aggregate interactions differs in 2 respects from typical immersional data: (a) the energy released is much greater, and (b) the energy is released over a long period of time. In fact, little change is noted in tail height after 3 hours even when the reaction has been followed for 24 hours. Both observations deserve comment.

For comparative analysis, the following immersional energies are cited (14): liquid, energy in ergs/cm^2 for water, 261; benzene, 218; n-octane, 185; cyclohexane, 68; and methanol, 185. Comparing these values with the immersional curves, we observe that within a few minutes the energy released is much greater than any of those values presented for simple liquids. Because asphalt contains a greater variety of polar groups than are represented by this short list, other functional groups present in asphalt could be principal contributors to the immersional energy. But even with this consideration, the large amount of energy released cannot be explained by monolayer wetting. What is the source of this large immersional energy? It is either (a) a chemical reaction catalyzed by the surface, or (b) physical adsorption not just of a monolayer but of a multilayer buildup.

The amount of energy released in the asphalt-aggregate interaction is proportional to the surface area; therefore, if a chemical reaction is occurring, it is surface catalyzed and the flat tail of the curve indicates the reaction is diffusion controlled.

A second possible explanation of the shape of the curves is that a monolayer produces the peak and a multilayer buildup produces the tail. This postulation would lead one to

expect greater peak heights to be accompanied by greater tail heights. Examination of the curves shows this is not so. With the limited asphalt-aggregate immersion data, an explanation of this anomaly is difficult.

Comparative analysis of the curves and strip tests shows the tail height correlates better with resistance to stripping than does the peak height. This statement is supported by the Montana aggregate immersion curves for both untreated and amine salt-treated asphalts.

Henniker (15) has presented a comprehensive list of examples where multilayer formation has been observed. He states, "The concept is therefore that, although the powerful forces are of very short range, they are transmitted by successive polarization of neighboring molecules to an impressive depth.... The effective depth of the surface zone is tens or hundreds in low molecular weight liquids, thousands of angstroms in long-chain molecules."

The molecular "melting-pot" mixture of asphalt includes not only long-chained molecules but also polar ring compounds of various types. The combination of high molecular weight compounds and an abundance of polar groups would enhance multilayer formation.

Whether the long tail on the curves represent multilayer buildup or not, the area under the curve definitely appears to be related to adhesion. More microcalorimetric work is needed to probe farther into the phenomena of asphalt-aggregate interactions.

ACKNOWLEDGMENTS

The authors wish to thank Stephen Weber for stimulating discussions and helpful suggestions and John Cavanaugh for assistance in data acquisition and calculations. This research was performed at Montana College of Mineral Science and Technology.

REFERENCES

1. Mack, C. In Bituminous Materials, Asphalt Tars and Pitches (Hoiberg, A. J., ed.), Interscience Publishers, New York, Vol. 1, 1964, p. 25.
2. Bikerman, J. J. Jour. of Materials, Vol. 1, No. 1, 1966, p. 34.
3. Dron, R. P. In Contact Angle Wettability and Adhesion, American Chemical Soc., Washington, D.C., Advances in Chemistry Series, No. 43, 1964, p. 310.
4. Barth, E. J. Asphalt Science and Technology. Gordon and Breach, New York, 1962.
5. Brown, B. W., and Welby, C. W. Improvement of Sands and Gravels for Use With Asphalts. Univ. of Southern Mississippi, Final Report.
6. Zettlemoyer, A. C. In Chemistry and Physics of Interfaces (Ross, S., ed.), American Chemical Soc., Washington, D.C., 1965.
7. Calvet, E., and Prat, H. In Recent Progress in Microcalorimetry (Skinner, H. A., transl. and ed.), Macmillan Co., New York, 1963.
8. Wilson, W. H., and Epps, T. D. Phys. Soc., London, Proc. Vol. 32, 1920, p. 326.
9. Gier, J. T., and Boelter, L. M. K. In Temperature, Its Measurement and Control in Science and Industry, Reinhold Publishing Co., New York, 1941.
10. Benzinger, T. H., and Kitzinger, C. In Temperature, Its Measurement and Control in Science and Industry, Reinhold Publishing Co., New York, 1963.
11. Bikerman, J. J. Surface Chemistry. Academic Press, New York, 1966.
12. Electro-Chemical Reactions in an Aggregate-Asphalt System-Research Project. Montana State Highway Commission, Helena.
13. Karius, H., and Dalton, J. L. Jour. Inst. Petrol, Vol. 50, No. 481, 1964, p.1.
14. Bartel, F. E., and Sugitt, R. M. Jour. Phys. Chem., Vol. 58, No. 36, 1954.
15. Henniker, J. C. Rev. Mod. Phys., Vol. 21, 1949, p. 322.